How to Overcome mmWave Automotive Radar Testing Challenges p27

What Do You Prefer When OTA Testing 5G mmWave Devices: DFF or CATR? p36

These Peak Power Sensors Go Beyond Making Basic Power Measurements p40

Microwaves & RF®

YOUR TRUSTED ENGINEERING RESOURCE FOR OVER 50 YEARS

MARCH 2019 mwrf.com

Taking 5G Test to the Field

Fitted with a powerful color touchscreen, these spectrum analyzers reach 54 GHz p67

$10.00


3H Communication Systems
ACCOMPLISH
YOUR MISSION
WITH THE SMALLEST
MOST COST EFFECTIVE
CUSTOM RF/MICROWAVE
FILTERS
Miniature SMT, Cavity Filters, available from 5.0 to 25 GHz
Nano, SMT Filters, available from 40 MHz to 6.0 GHz, in LC and Ceramic Topologies
Pico, SMT Filters, available from 5.0 GHz to 27 GHz
Miniature Filters, rated for Mil-Std-202; compliant with RoHS and NON-RoHS options.
Miniature Diplexers, available from 40 MHz to 27 GHz
When an off-the-shelf filter could compromise your mission, call on 3H Communication Systems for the support you need. 3H specializes in high-performance custom RF/microwave filter solutions from DC to 50GHz.
• Custom-designed to meet the most critical performance and size requirements
• 3H has extensive experience with defense and prime contractors
• Cavity, Lumped Component and Ceramic topologies, connectorized and/or SMT formats; printed, suspended substrate, switch filter banks and multi-function assemblies
• ISO9001:2015 certified facilities with products backed by 5-year warranty
3H Communication Systems
Learn more about how 3H can keep your project on track by talking to one of our engineers.
Call 949.529.1583 or visit 3HCommunicationSystems.com.

Ultra Low Phase Noise

Phase Locked Clock Translators

Up to 3.0 GHz

Model	Frequency	Ref. Input	DC Bias	Typical Phase Noise (dBc/Hz)				Package
	(MHz)	(MHz)	(VDC)	100 Hz	1 kHz	10 kHz	100 kHz	
FCTS800-10-5	800	10	+5, +12	-87	-116	-144	-158	
KFCTS800-10-5	800	10	+5, +12	-87	-116	-144	-158	
FCTS1000-10-5	1000	10	+5, +12	-75	-109	-140	-158	
FCTS1000-10-5H	1000	10	+5, +12	-84	-116	-144	-160	
FCTS1000-100-5 *	1000	100	+5, +12	-75	-109	-140	-158	
KFCTS1000-10-5 *	1000	10	+5, +12	-75	-109	-140	-158	
FCTS2000-10-5 *	2000	10	+5, +12	-80	-105	-135	-158	
FCTS2000-100-5 *	2000	100	+5, +12	-80	-105	-135	-158	
KFCTS2000-100-5 *	2000	100	+5, +12	-80	-105	-135	-158	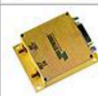
FSA1000-100	1000	100	+3.3, +5, +12	-105	-115	-145	-160	
KFSA1000-100	1000	100	+12	-105	-115	-145	-160	
FXLNS-1000	1000	100	+5, +12	-120	-140	-149	-154	
KFXLNS-1000	1000	100	+12	-120	-140	-149	-154	

** New for 2018*

Features

- Cost Effective
- Replaces Noisy Frequency Multipliers
- No Programming Required
- Lead Free RoHS Compliant

Applications

- Scanning & Radar Systems
- ADC & DAC Fast Clocking & Sampling
- Test & Measurement Equipment
- High Performance Frequency Converters
- Base Station Applications
- Front End Converter LO's

Talk To Us About Your Custom Requirements.

SYNERGY®
MICROWAVE CORPORATION

Phone: (973) 881-8800 | Fax: (973) 881-8361
E-mail: sales@synergymwave.com | Web: www.synergymwave.com
Mail: 201 McLean Boulevard, Paterson, NJ 07504


Mitutoyo
MADE IN JAPAN
Infinity Probe

IN THIS ISSUE

FEATURES

36

40

67

78

NEWS & COLUMNS

defense electronics

Starts on page **49**

JOIN US ONLINE

follow us @MicrowavesRF

become a fan at facebook.com/microwavesRF

RF SWITCHES

DC - 40 GHz

Type	Failsafe	Latching	Normally Open	Terminations	SMA	2.92mm	Type-N	7/16, 4.3-10	SC	High Power (CW)	Low PIM (dBc)	Cycle Life
SPDT	✓	✓	✓	50Ω, 2W	✓	✓	✓	✓	✓	2kW	-170	5M
Transfer	✓	✓			✓	✓	✓	✓	✓	2kW	-170	5M
SPMT*	✓	✓	✓	50Ω, 2W	✓	✓	✓	✓	✓	2kW	-170	5M

***SP3T to SP12T designs**

Visit www.e360microwave.com for data sheets and more information.

e360microwave offers relays and switches for ultra reliable test applications. Based on a 30-year heritage of innovative RF and microwave products and designs, our broad selection of relays and switches features excellent RF performance, reliability and repeatability. We can deliver 10,000s switches per month, quickly and at very competitive prices. All options are available and high-power and low PIM designs are a specialty.

e360 microwave

Santa Clara, CA 95054 408-650-8360 (o), 408-650-8365 (f)

techsupport@e360microwave.com

sales@e360microwave.com

RoHS Compliant REACH COMPLIANCE ISO 9001

ON MICROWAVES&RF.COM

What's the Difference Between the Four Stratum Levels?

Bliley's Rob Rutkowski discusses stratum clock systems and then explains what's behind each of these stratum levels in the Network Time Protocol.

https://www.mwrf.com/systems/what-s-difference-between-four-stratum-levels

Striking the Right Balance: RF Power Output and Efficiency

Optimizing the cost and operating time for portable electronic systems running on batteries often comes down to one critical system-level parameter: efficiency.

https://www.mwrf.com/components/striking-right-balance-rf-power-output-and-efficiency

Calibration Techniques for Phased-Array Antennas

This latest "Algorithms to Antenna" blog post discusses calibration for perturbed phased-array antennas, examining techniques like pilot calibration and self-calibration.

https://www.mwrf.com/systems/algorithms-antenna-calibration-techniques-phased-array-antennas

What You Need to Know About Radio Telescopes

In his Line of Sight blog, Lou Frenzel explores how extreme, leading-edge radio technology, including very large arrays and massive dishes, enable advanced space research.

https://www.mwrf.com/systems/what-you-need-know-about-radio-telescopes

join us online

twitter.com/MicrowavesRF facebook.com/microwavesrf

CHRIS DeMARTINO | Technical Editor
chris.demartino@informa.com

An Illuminating Look at the Current RF Landscape

With the likes of 5G and more, there's no question that test-and-measurement companies are faced with meeting many new challenges. One company right in the thick of it is Rohde & Schwarz *(www.rohde-schwarz.com)*, a familiar name to anyone in the RF/microwave industry. To explain some of today's significant and challenging applications, Rohde & Schwarz hosted the RF LUMINATION 2019 event on February 21. In the company's own words, this one-day event was created to "lay the groundwork for RF test and measurement and bridge the gap between the visions of what could be to the implementation of what will be."

RF LUMINATION 2019 included a keynote presentation along with eight technical classes. Instructors for the technical sessions consisted of Rohde & Schwarz personnel along with representatives from Focus Microwaves *(www.focus-microwaves.com)*, Integrated Device Technology (IDT; *www.idt.com*), and Texas Instruments *(www.ti.com)*.

5G was clearly a focal point of the event. The keynote, given by Andreas Roessler, Technology Manager at Rohde & Schwarz, focused in on 5G topics like key parameters, link budgets, hybrid beamforming, over-the-air (OTA) testing, and more. Of course, Roessler mentioned some specific R&S instruments along the way.

Among the eight technical sessions was one titled, "Automated RF Component Test for Design Engineers Without Programming." The presentation, given by Martin Lim, national applications engineer at Rohde & Schwarz, centered on how test automation can be made easier. Lim explained that R&S is simplifying test automation, as many common tasks can be automated inside the instrument itself. The presentation was divided into three sections, focusing in on an amplifier amplification before discussing what Lim described as "in-the-box automation" followed by custom automation.

Another technical session, "Advanced Techniques for Phase Noise and Jitter Measurements," was presented by Rohde & Schwarz's Greg Bonaguide. In this session, Bonaguide first discussed the basics of phase noise before talking about its importance along with various phase-noise measurement techniques. Those with an interest in phase noise will likely want to check out this presentation.

The remaining workshops covered 5G millimeter-wave (mmWave) chipset characterization using on-wafer load-pull, digital Doherty power amplifiers, residual (additive) phase-noise measurements, phased-array antennas, multiple-input, single-output (MISO) transmitters, and wideband multi-antenna applications with data-converter integration.

Those interested can visit the RF LUMINATION 2019 website to view the keynote and technical sessions. mw

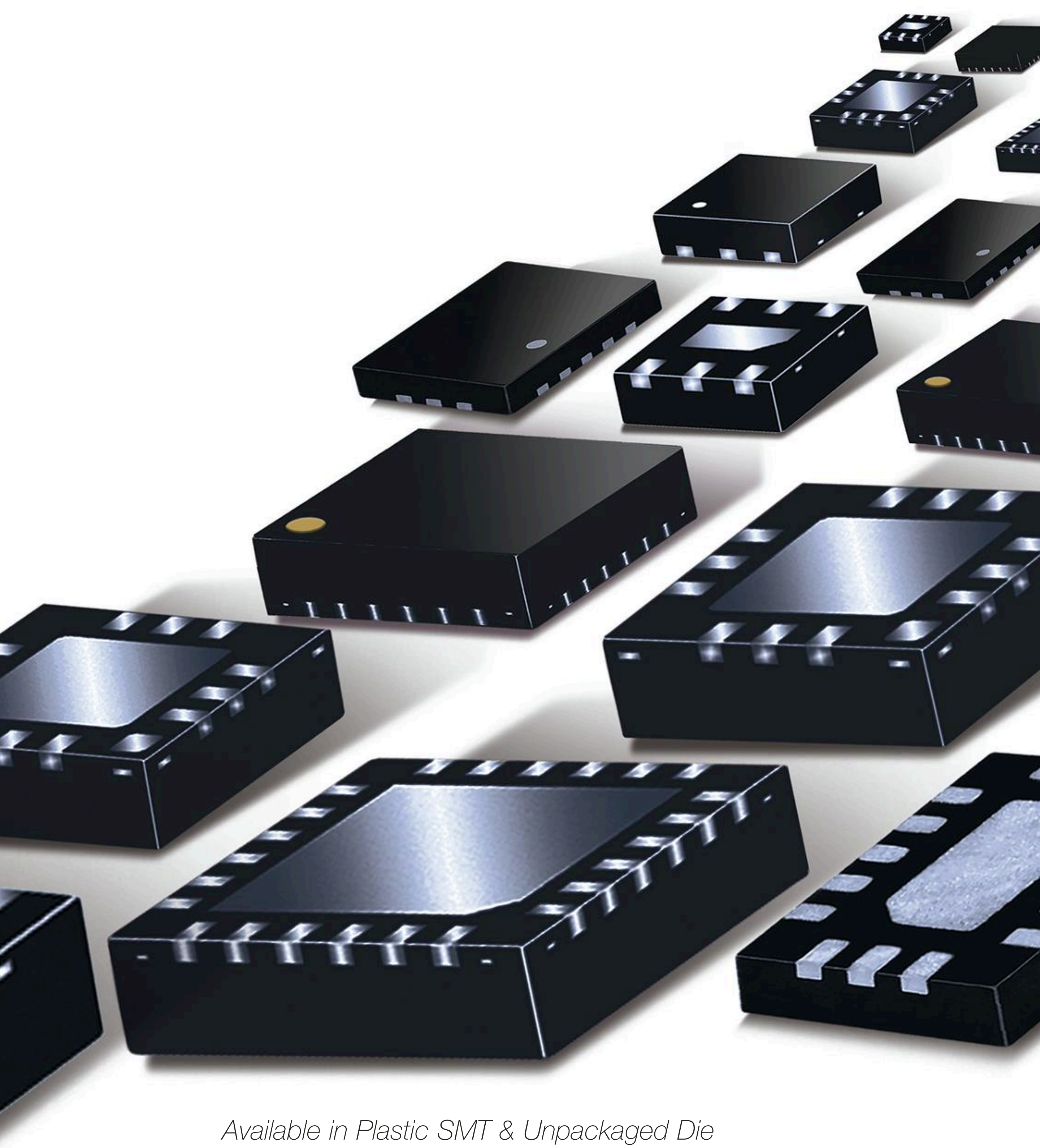

Available in Plastic SMT & Unpackaged Die

Microwaves&RF **MARCH 2019**

EDITORIAL

EXECUTIVE DIRECTOR, CONTENT: **KAREN FIELD** karen.field@informa.com
TECHNICAL CONTRIBUTOR: **JACK BROWNE** jack.browne@informa.com
TECHNICAL ENGINEERING EDITOR: **CHRIS DeMARTINO** chris.demartino@informa.com
ASSOCIATE EDITOR/COMMUNITY MANAGER: **ROGER ENGELKE** roger.engelke@informa.com
ASSOCIATE EDITOR/COMMUNITY MANAGER: **JEREMY COHEN** jeremy.cohen@informa.com
ASSOCIATE CONTENT PRODUCER: **JAMES MORRA** james.morra@informa.com

ART DEPARTMENT

GROUP DESIGN DIRECTOR: **ANTHONY VITOLO** tony.vitolo@informa.com
CONTENT DESIGN SPECIALIST: **JOCELYN HARTZOG** jocelyn.hartzog@informa.com
CONTENT & DESIGN PRODUCTION MANAGER: **JULIE JANTZER-WARD** julie.jantzer-ward@informa.com

PRODUCTION

GROUP PRODUCTION MANAGER: **GREG ARAUJO** greg.araujo@informa.com
PRODUCTION MANAGER: **VICKI McCARTY** vicki.mccarty@informa.com

AUDIENCE MARKETING

USER MARKETING MANAGER: **DEBBIE BRADY** debbie.brady@informa.com
FREE SUBSCRIPTION / STATUS OF SUBSCRIPTION / ADDRESS CHANGE/ MISSING BACK ISSUES:
OMEDA **T** | 847.513.6022 **TOLL FREE** | 866.505.7173

SALES & MARKETING

MANAGING DIRECTOR: **TRACY SMITH** **T** | 913.967.1324 **F** | 913.514.6881 tracy.smith@informa.com
REGIONAL SALES REPRESENTATIVES:
AZ, NM, TX: **GREGORY MONTGOMERY** **T** | 480.254.5540 gregory.montgomery@informa.com
AK, NORTHERN CA, OR, WA, WESTERN CANADA: **STUART BOWEN** **T** | 425.681.4395 stuart.bowen@informa.com
AL, AR, SOUTHERN CA, CO, FL, GA, HI, IA, ID, IL, IN, KS, KY, LA, MI, MN, MO, MS, MT, NC, ND, NE, NV, OH, OK, SC, SD, TN, UT, VA, WI, WV, WY, CENTRAL CANADA: **JAMIE ALLEN** **T** | 415.608.1959 **F** | 913.514.3667 jamie.allen@informa.com
CT, DE, MA, MD, ME, NH, NJ, NY, PA, RI, VT, EASTERN CANADA:
ELIZABETH ELDRIDGE **T** | 917.789.3012 elizabeth.eldridge@informa.com

INTERNATIONAL SALES:
GERMANY, AUSTRIA, SWITZERLAND: **CHRISTIAN HOELSCHER** **T** | 011.49.89.95002778
christian.hoelscher@husonmedia.com
BELGIUM, NETHERLANDS, LUXEMBURG, UNITED KINGDOM, SCANDINAVIA, FRANCE, SPAIN, PORTUGAL:
JAMES RHOADES-BROWN **T** | +011 44 1932 564999 **M** | +011 44 1932 564998 james.rhoadesbrown@husonmedia.com
ITALY: **DIEGO CASIRAGHI** diego@casiraghi-adv.com
PAN-ASIA: **HELEN LAI** **T** | 886 2-2727 7799 helen@twoway-com.com
PAN-ASIA: **CHARLES LIU** **T** | 886 2-2727 7799 liu@twoway-com.com

PLEASE SEND INSERTION ORDERS TO: orders@informa.com
INFORMA REPRINTS: **WRIGHT'S MEDIA** **T** | 877.652.5295
LIST RENTALS/ SMARTREACH CLIENT SERVICES MANAGER: **MARY RALICKI** **T** | 212.204.4284
mary.ralicki@informa.com

DIGITAL

GROUP DIGITAL DIRECTOR: **RYAN MALEC** ryan.malec@informa.com

DESIGN ENGINEERING & SOURCING GROUP

EXECUTIVE DIRECTOR, CONTENT: **KAREN FIELD** karen.field@informa.com
VP OF MARKETING: **JACQUIE NIEMIEC** jacquie.niemiec@informa.com

INFORMA MEDIA INC.

605 THIRD AVENUE
NEW YORK, NY 10158 USA **T** | 212.204.4200

informa

Electronic Design | Machine Design | Microwaves & RF | Source ESB | Hydraulics & Pneumatics | Global Purchasing | Distribution Resource | Power Electronics | Defense Electronics

News

DC ENERGY ANALYZER

Finds its Way to Kickstarter

One upcoming test-related product that may pique your interest is Joulescope (www.joulescope.com), a precision dc analyzer that can measure current and voltage and then compute power and energy *(Fig. 1)*. Joulescope was created by Jetperch *(www.jetperch.com)*, an engineering services company focused on hardware and software development for various industries.

Joulescope was developed so that users could quickly and easily optimize the energy consumption and battery life of a target device. Instantaneous voltage, current, power, and energy readings can be displayed when using Joulescope. And, like an oscilloscope, waveforms of voltage and current over time can be viewed *(Fig. 2)*.

So what was the genesis of Joulescope? Matt Liberty, the creator of Joulescope, explains, "At numerous times during my career and across different projects, I struggled to accurately and affordably measure current and energy consumption. Having easy access to this information during product development is crucial, especially for battery-powered devices. Two years ago, I started to develop Joulescope to solve this problem."

Today, as the number of Internet of Things (IoT) products rapidly increases, it's even more critical to accurately measure energy consumption. Specifically, many IoT products and other battery-powered devices have a high dynamic current range, meaning the devices consume current in the nanoamp (nA) or microamp (µA) range when "sleeping." When active, these devices consume current in the milliamp (mA) or amp (A) range. Joulescope is well-suited for these scenarios, as it combines high-speed sampling with high dynamic range to make accurate measurements—even for devices with rapidly varying current consumption.

To use Joulescope, one must connect it to a PC with a USB cable. The Joulescope host software, which can be downloaded from the website and is open source on GitHub, will automatically detect the connected instrument. The IN port connects to the power source, while the OUT port connects to the device under test (DUT). Upon operating the DUT, measurements can then be displayed via the host software.

As mentioned earlier, Joulescope delivers high-speed sampling capability. Specifically, it can measure current and voltage two million times per second with a 250-kHz bandwidth. Another benefit of Joulescope is the total voltage drop is only 25 mV at 1 A, thereby allowing target devices to continue functioning correctly. And Joulescope's fast current-range switching maintains a low voltage drop—even under rapidly varying current demands.

Joulescope launched February 19 on Kickstarter with a starting price tag of $399, a significant discount from the $799 retail price. Shipments will begin in June 2019.

Those interested can visit the Joulescope Kickstarter page *(http://kck.st/2BIKIcJ)*. ■

1. The Joulescope energy analyzer represents the culmination of nearly two years of work.

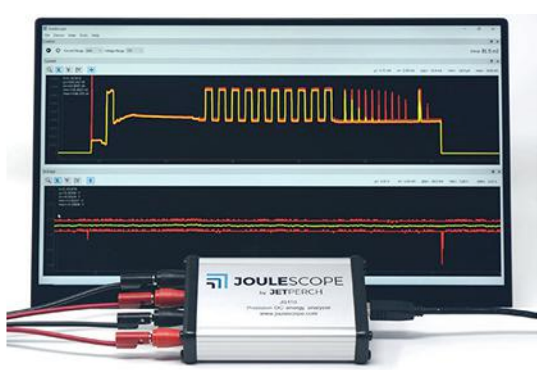

2. With Joulescope, it's possible to make oscilloscope-like measurements.

ARRA Sports a New Website

ARRA (WWW.ARRA.COM), a supplier of RF/microwave components, recently launched its new website. The goal was to make it easy for visitors to navigate through the company's assortment of products. ARRA offers both coaxial and waveguide components, with products like attenuators, phase shifters, couplers, power dividers, and switches, among others. The new website simplifies the navigation to individual pages for each of ARRA's product lines, enabling visitors to obtain more detailed information like specifications and other performance data.

ARRA, which has been in business for over 60 years, is located in Bay Shore, N.Y. ■

WIDEBAND MICROWAVE TRANSCEIVER Strives for Versatility

MERCURY SYSTEMS (WWW.MRCY.COM) recently announced that it shipped its first SpectrumSeries RFM3101 wideband microwave transceiver to a supplier of electronic-warfare (EW) systems. This announcement came after the company showcased the RFM3101 at the annual Association of Old Crows (AOC) International Symposium and Convention last November. With this transceiver innovation, the company further leverages its proficiency across a wide range of engineering disciplines. The product is the end result of a collaboration of teams from several Mercury locations.

Supplied in a 3U form factor, the RFM3101 is a 6- to 18-GHz transceiver with an intermediate-frequency bandwidth (IFBW) that spans 1.375 to 2.375 GHz *(see figure).* Open-systems compliance is a major aspect of the RFM3101, as the transceiver is compliant with the OpenVPX specification. In addition, the RF modules housed inside are OpenRFM-compliant. While EW applications are expected to be a prime area of use for the RFM3101, the transceiver can also enable other applications, such as spectrum monitoring and beamforming.

"The RFM3101 is a 3U OpenVPX module," says Brian Kimball, senior product manager at Mercury Systems. "In order to maximize system flexibility, the transceiver includes two interfaces for OpenRFM modules—we call them 'slim slices' or 'bricks.' In its standard configuration, one module is a receiver and one is a transmitter. Additionally, we can easily mix and match the modules to support other applications. For example, we also have a dual-receiver version that consists of two down-conversion modules. The beauty of OpenRFM is that you can utilize both 3U and 6U sizes. With 6U, you can actually fit five slim slices as opposed to two with 3U OpenVPX."

In terms of the RFM3101's functionality, Kimball adds, "There are phase-locked loops (PLLs) onboard. It's also possible for local oscillators (LOs) to go in and out of the bricks. So, you could have a DDS-based synthesizer or some fast-tuned capability in which you daisy-chain these LOs across modules for coherent tuning and exciting. You can also daisy-chain references—the bricks have reference inputs and outputs so that you can use the onboard PLLs to generate the LOs."

Both the upconverter and downconverter RF modules deliver 20 dB of gain. They can be set to an attenuation level as high as 31 dB in 0.5-dB step sizes. In addition, the downconverter achieves an output 1-dB compression (P1dB) of +15 dBm at the maximum gain setting, while the upconverter attains a P1dB of +21 dBm with maximum gain. ■

The RFM3101 wideband transceiver maintains an RF frequency range of 6 to 18 GHz.

SPECTRUM SALES Named Mini-Circuits' Rep

MINI-CIRCUITS has added long-time industry sales representative Spectrum Sales *(www.spectrumsales.com)* to handle sales in the New York, northern New Jersey, and southern Connecticut region. For over 55 years, Spectrum Sales has built an organization that provides practical design support for the companies it represents, providing guidance on active and passive RF/microwave components, materials, and subsystems.

Working with commercial, industrial, military, and high-reliability (HiRel) customers, Spectrum Sales helps with the specification process. It represents an impressive lineup of companies, including Bliley, Comtech PST, Guerrilla RF, L3 Narda/MITEQ, and now Mini-Circuits with its large product catalog.

Spectrum Sales Inc. (SSI) will help Mini-Circuits customers through its staff of experienced sales engineers who have extensive backgrounds in RF/microwave component, circuit, and system design, as well as measurement techniques. The sales representative also handles related technologies and supporting products/manufacturers, such as digital and fiber-optic components and materials, to aid high-frequency design customers in achieving practical, multiple-function solutions. The website provides categorization of technical areas by major component types and materials, for ease of navigation. ■

SPECTRUM SALES INC. (SSI), P.O. Box 369, Syosset, NY 11791; (516) 921-5750, FAX: (516) 921-5776, E-mail: sales@spectrumsales.com, www.spectrumsales.com

QUALCOMM Introduces its First Multimode 5G Modem

QUALCOMM, THE LARGEST SUPPLIER of smartphone chips, introduced its second-generation modem for tapping into 5G networks, which are projected to have speeds 10 to 100 times faster than current LTE networks. The company said the modem is designed to be faster, smaller, more power efficient and able to handle a broad range of frequency bands. The announcement came ahead of the Mobile World Congress in Barcelona last month.

The Snapdragon X55 is manufactured on the 7-nanometer node, while the first generation of the modem, the X50, is based on 10-nanometer technology. Qualcomm's X55 modem stands out for inte-

When Everything is Important...
the NEW *Clarity™ Series* is the *Clear Choice*

Applications:

Research & Development Labs
VNA Test Port Extension Cables
High Volume Production Test
Bench or Portable Test equipment
RF Module Testing

Industry leading performance, unparalleled value, and stock to 4-week lead times.

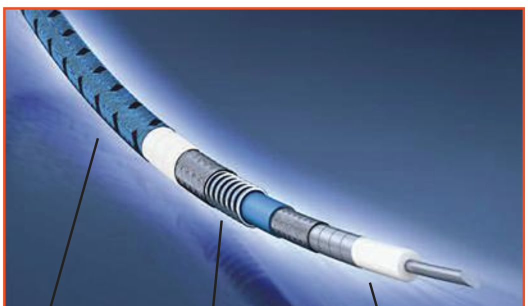

Phase stability <3.5º
Guaranteed up to 50,000 flexes
Super-sharp Sure-Grip™ knurl
Ergonomically designed Sure-Grip™ molding

TIMES MICROWAVE SYSTEMS
An Amphenol Company

World Headquarters: 358 Hall Avenue, Wallingford, CT 06492 • Tel: 203-949-8400, 1-800-867-2629 Fax: 203-949-8423
International Sales: 1+ 203 949 8503 • 1+ 800 867 2629
China Sales: TMC Building 4, No. 318 Yuanshan Road, Xinzhuang Industrial Park, Shanghai, China 201108 Tel: 86-21-5176-1209 Fax: 86-21-64424098

www.timesmicrowave.com

grating all the technology for tapping into 2G, 3G, 4G and 5G networks on the same flake of silicon. Even though customers are building the X50 modem into smartphones due out before the end of the year, the first-generation chip can only handle 5G.

Because the X50 modem is limited to 5G technology, the chip needs to be combined with the modem inside Qualcomm's Snapdragon 855 processor to access 2G, 3G and 4G networks. Conversely, the multimode X55 modem consumes less power, takes up less board space and costs less to integrate into devices, according to Qualcomm. Curbing costs is critical because the first 5G smartphones could end up being pricier than 4G models.

The second generation modem is also faster than the X50, which was introduced when the 5G standard was still under development in 2016. The chip delivers peak download speeds of 7 Gb/s using 5G networks, or 40 percent faster than the X50, which downloads data as fast as 5 Gb/s. The maximum upload speed is 3 Gb/s. Using 4G networks, the chip is capable of 2.5-Gb/s downloads, or 25 percent faster than Qualcomm's X24 LTE modem.

The X55 modem can support both non-standalone and standalone 5G networks, which operate in sub-6 GHz frequency bands—the same used by LTE—and millimeter-wave frequencies that have greater network capacity. The chip covers "virtually any 5G network or region in the world," according to Qualcomm. The product also has a spectrum-sharing mode that allows 4G and 5G services to run on the same radio frequencies at the same time.

Qualcomm is betting on the speed of 5G networks to drum up slowing smartphone sales. The company's growth has slumped at a time when it remains under scrutiny from the Federal Trade Commission for allegedly holding a monopoly in the modem business. The 33-year-old company is also fighting Apple over how it licenses standard essential wireless patents and facing mounting competition from Intel, Mediatek, and some customers.

Last year, Intel said that its latest multimode 5G modem could support maximum speeds of 6 Gb/s. The Silicon Valley company said the XMM8160 would be used in smartphones by the first half of 2020. Last year, Apple forced Qualcomm out of its flagship smartphones in favor of Intel, which now makes the modem used in every iPhone. Before losing half its orders to Intel in 2017, Qualcomm was the exclusive supplier of modems used in the iPhone.

Mediatek, which typically targets lower end smartphones than Qualcomm, announced its M70 cellular modem last year with 5-Gb/s download speeds. The chip should start shipping the second half of 2019, the company said. Mediatek, Intel and Qualcomm's products are all discrete modems, meaning they are not actually built into the application processor. Mediatek and Qualcomm can only currently build 4G modems directly into SoCs.

Qualcomm is also facing fresh competition from potential customers. Huawei's HiSilicon unit announced its first 5G multimode modem, the Balong 5000, based on 7-nanometers in January. Samsung's 10-nanometer Exynos 5100 cellular modem is designed for Samsung devices sold in regions other than the United States. Samsung partnered with Qualcomm last year to release a phone powered by the X50 modem targeting consumers in the U.S.

Wrestling with Qualcomm in courts around the world, Apple is hiring radio frequency engineers to create a custom modem for future iPhones, taking Intel out of the equation. Nearly two years ago, Apple poached the engineering executive that had been leading Qualcomm's modem chip development, Esin Terzioglu. The plan could hurt Qualcomm's chances of reviving its relationship with Apple once their legal conflicts simmer down.

Still, the San Diego, California-based company is winning over early customers. Qualcomm's X55 modem should start shipping inside commercial devices by the end of 2019, the company said. The 5G cellular chip is also targeted at applications such as personal computers, cars, and wireless routers. In January, the company said that the first-generation

(Continued on page 77)

MINIATURIZING ANTENNAS with Magnetic Materials

ANTENNAS ARE THE beginning and ending points for many systems and with a growing number of wireless applications, there's a greater demand for efficient, miniature low-profile antennas. In pursuit of such components, Evmorfili Andreou and three fellow researchers from Athens, Greece have explored the use of magnetodielectric materials with tunable permeability for reconfigurable antenna designs.

Magnetodielectric materials exhibit relative permittivity (ε_r) and relative permeability (μ_r) of greater than one. By using a magnetodielectric substrate material with moderate values of permittivity and permeability, it's possible to miniaturize an antenna as much as when using a dielectric substrate material with a considerably higher value of ε_r.

The researchers noted the constant need for antennas capable of adjusting operating characteristics to adapt to changing channel conditions. Tunable materials such as ferroelectric and ferromagnetic substrates can provide excellent starting points for wideband antenna designs, especially magnetic materials with high resistivity for high-frequency antennas.

Ferrimagnetic oxides have unique properties when a magnetic field is applied, making them suitable for antennas and other microwave components. Ferrimagnetic oxides, with iron oxide as their main component, are classified as spinels, garnets, and hexaferrites. Garnets are typically employed for components from 1 to 10 GHz, spinels are commonly used for applications from 3 to 30 GHz while hexaferrites are used for higher-frequency designs, as high as 100 GHz. Ferrites typically have high permittivity and low dielectric losses, with flexible magnetic properties.

When modeling the properties of ferrimagnetic materials, such as permeability, magnetic flux density, magnetic field strength, and resonance linewidth, it's the magnetic bias field that controls the switching of the material between two magnetization states. For example, different materials can be considered partially magnetized or magnetically saturated, and the approach to simulating this parameter will differ for the various ferrimagnetic materials.

The researchers explain their approach to simulating the different materials and choosing a ferrimagnetic material for a reconfigurable antenna design. Material selection depends on the target frequency range of the antenna. Simulation with electromagnetic (EM) modeling software involves computing material parameters, such as permeability, in the "off" and "on" states of the material (without and with magnetic field applied). By dividing their yttrium iron garnet (YIG) material sample into different zones for study, the magnetic field distribution can be precisely calculated. The modeled antenna performance from approximately 4.6 to 5.5 GHz closely matches the measured performance for a fabricated component.

See "Magnetodielectric Materials in Antenna Design," *IEEE Antennas & Propagation Magazine*, Vol. 61, No. 1, February 2019, pp. 29-40.

IMPROVING WiMAX Reception at 3 GHz

AS THE POPULARITY of wireless communications systems, such as WiMAX, continues to grow worldwide, antenna designers are faced with making components that are smaller but provide better reception than their older, larger predecessors. In quest of such a next-generation WiMAX antenna, Rajkishor Kumar, Sreenath Reddy Thummaluru, and Raghvendra Kumar Chaudhary from the Indian Institute of Technology in Dhanbad, India developed a dielectric resonator antenna (DRA) using a stair-shaped microstrip feed line, a rectangular dielectric resonator (DR), and a pair of L-shaped slots in the ground plane. The feed line enables the antenna to achieve wideband frequency coverage (2.94 to 3.85 GHz) with a circularly polarized (CP) radiation pattern.

The researchers followed a regimented, five-step design procedure to create the antenna. Slots in the ground plane were introduced as all antenna design parameters were kept constant by making modifications in the microstrip feed lines with the changes in the ground plane. In quest of a wide impedance bandwidth, several antenna designs were implemented until the target impedance bandwidth was achieved, modeling the amount of coupling between the DR and microstrip lines. Adding the L-shaped slot in the ground plane impacts the surface current density of the antenna design—parameters such as the height of the L-shaped slot affect the resonance mode on CP and the antenna's ultimate frequency range.

While the mechanical adjustments made to this DRA may initially seem elaborate, the fabricated antenna design is less complex than many standard WiMAX antennas that were used for reference comparison. The new design provides a usable bandwidth of better than 17% at the center frequency with a single DR compared to other rectangular and comb-shaped antennas with more than one resonator, far less bandwidth, and very complex implementation. It's also considerably smaller than the comparable WiMAX antenna designs, with better far-field parameters than the other reference antennas, for much improved WiMAX reception at greater distances.

See "Improvements in Wi-Max Reception," *IEEE Antennas & Propagation Magazine,* Vol. 61, No. 1, February 2019, pp. 41-49.

MARK ELO | Tektronix
www.tek.com

OVERCOME mmWave Automotive Radar Testing Challenges

With automotive radar moving to higher frequencies, the need exists for the right test solutions such as high-bandwidth oscilloscopes and versatile arbitrary waveform generators.

Recent regulation changes have allowed the automotive radar market to shift from the 24-GHz band to the 77-GHz band, introducing a range of new design and test challenges. Higher frequencies facilitate wider bandwidths and increasing resolution, while the shorter wavelengths provide smaller form factors and improved range enabled by a relaxation of the maximum power specification in the 77-GHz band. Better resolution, smaller size, and longer range mean that radar is rapidly becoming the sensor of choice for advanced driver-assistance systems (ADAS) and autonomous-vehicle applications.

This frequency shift, combined with the proliferation of sensors on vehicles, will drive a compound annual growth of 21% (CAGR) during the 2018 to 2022 timeframe, according to a recent market research report by Technavio.

Today, the modulation of choice for an automotive radar is linear frequency modulation (LFM) or frequency-modulated-continuous-wave (FMCW) radar. This type of modulation, often called "chirp," has roots that go back to the Cold War when electronic-warfare officers could often identify adversary radar by listening to the audio of the radar modulation. Different radar signatures would sound like different birds "chirping." Wide linear frequency sweeps equate to a higher-resolution radar.

Resolution in the case of radar means that two objects close to each other can be resolved—for example, being able to see the difference between a person standing near a lamp post, or two cars driving at the same speed very close together. In pulsed radar, shorter duration pulses provide better resolution. However, a short pulse is very hard to amplify.

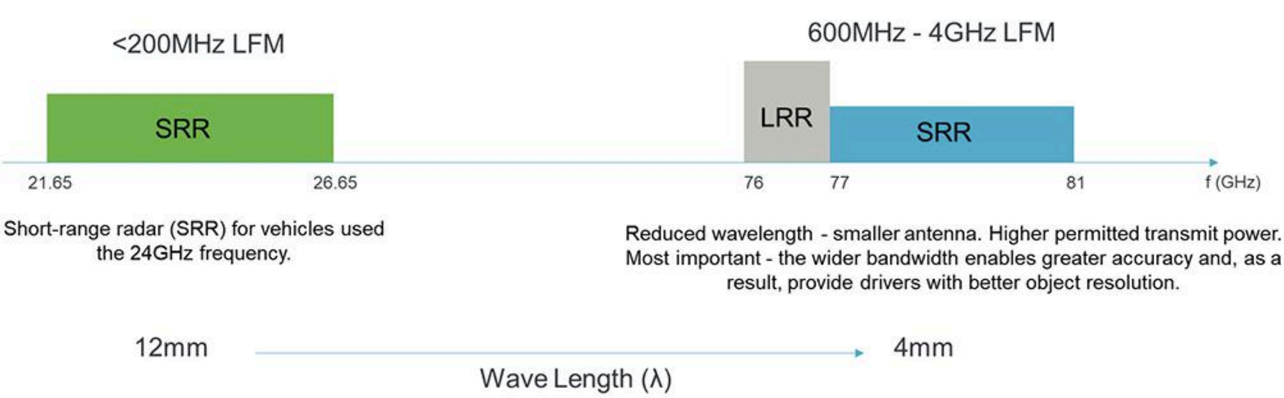

1. Moving from the 24-GHz band to the 76- to 81-GHz band enables more capability.

LFM is a way to overcome this problem. It's essentially a process of linearly increasing the frequency around a carrier. For example, if a center frequency is 77 GHz, a 4-GHz chirp—or LFM—effectively means linearly sweeping an RF carrier wave from 75 to 79 GHz in about 100 µs. The receiver "stacks" each element of the chirp by filtering and delaying the energy to create the equivalent of a very narrow pulse.

At 24 GHz, the maximum LFM is 600 MHz, which provides moderate range resolution and is adequate for long-range radar (LRR) applications. Because of this, it's predominantly used for adaptive-cruise-control applications. The new bands open up much higher bandwidths, enabling radar to be used for both LRR with chirps up to 1 GHz and short-range radar (SRR) applications with chirps up to 4 GHz, significantly increasing the vehicle's situational awareness while in motion.

As shown in *Figure 1*, another benefit of the higher frequency is that sensor size can be smaller. Wavelength is essentially inversely proportional to frequency. Therefore, the higher the frequency, the smaller the wavelength, which means the antenna can be literally one-third the size! This reduction is particularly useful for automotive applications in which sensors need to be mounted in tight spots behind the bumper or other locations around the car. Such locations include doors and trunks for proximity applications, as well as locations inside the car for in-cabin applications.

AUTOMOTIVE RADAR TECHNOLOGY

LFM, or FMCW, radar offers a very low-cost, compact, weather- and environment-tolerant way to get range and velocity from a target. Cost, size, and weight are key considerations for any automotive application.

In comparison to a pulsed radar employed in many military radars, FMCW radar saves considerable cost by essentially eliminating the pulse circuitry. The actual design is also relatively simple *(Fig. 2)*. A voltage-controlled oscillator (VCO) is used to generate the linear frequency ramp that's transmitted through the circulator. The transmit ramp is compared to the received ramp by using a mixer to subtract the two signals from each other. Post-signal processing, such as performing a fast Fourier transform (FTT) on the resultant signal, is then carried out in the processing and decision-making part of the system.

However, because no time reference exists with FMCW, range is harder to calculate than with pulsed radar, in which the pulses actually provide a time reference. For stationary targets, FMCW range is determined by measuring the linear frequency difference between transmit and receive. For automotive, of course, many targets are likely to be moving. If the target is moving, the receive frequency contains both the time-delayed frequency ramp of the chirp, plus a Doppler frequency offset.

To resolve moving targets, a second measurement is needed, such as chirp up (sweep frequency from low to high) and then chirp down (sweep frequency from high to low). This enables solving two simultaneous equations and extracting the Doppler information. This approach only works if there's a single moving target. To discriminate multiple targets, it's necessary to add an additional chirp type (sweep at a different rate, for example). By adding a new chirp and other frequency difference measurements after the chirp up and chirp down ramp to the modulation scheme, it's possible to solve the equations for the real targets.

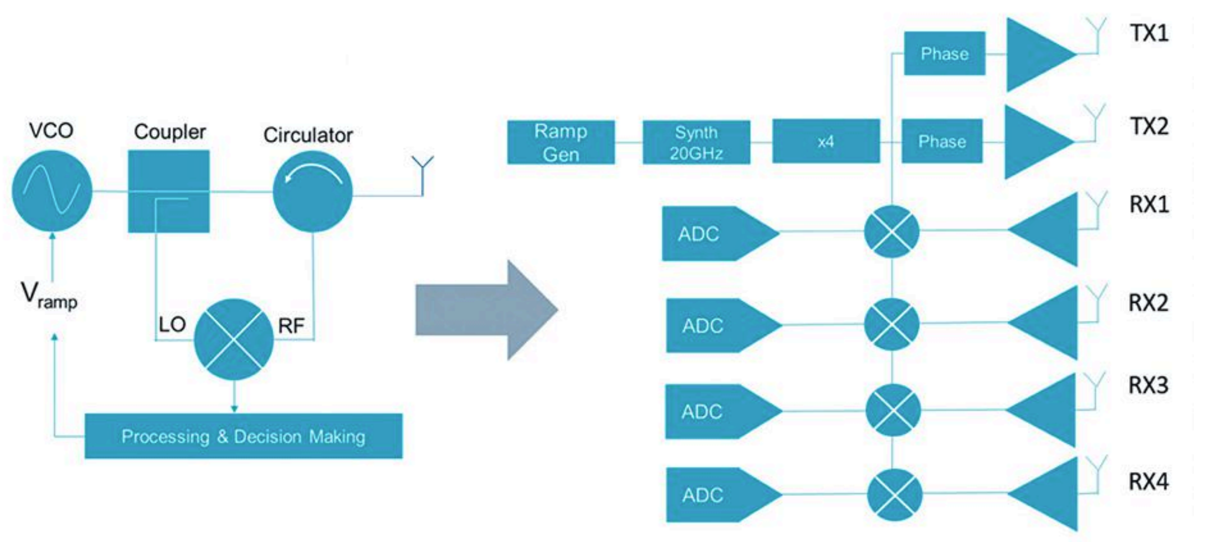

2. An FMCW radar is a relatively simple concept. Adding multiple transmit and receive channels helps create an appropriate beam width or wave front and determine angle of arrival.

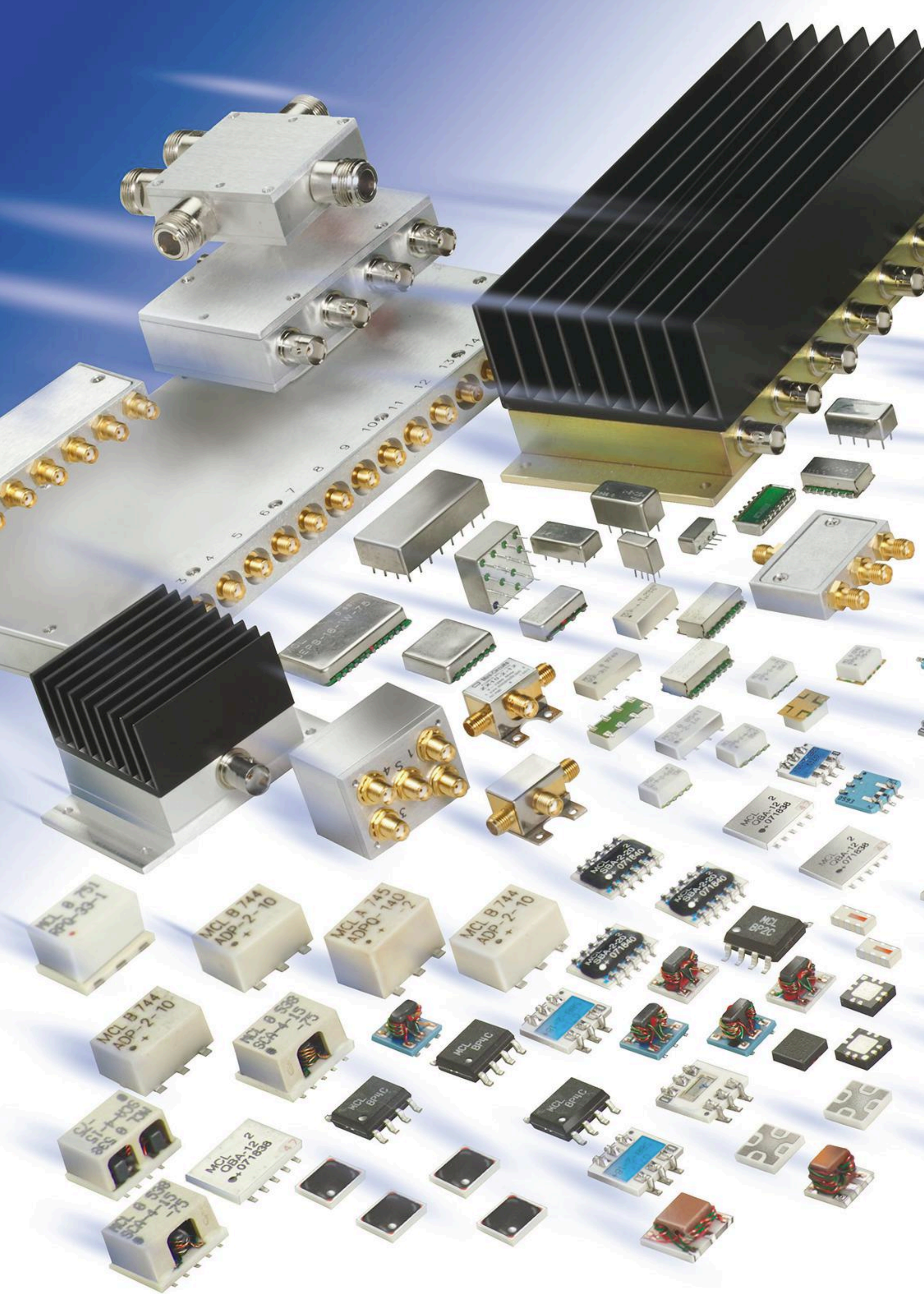

MCL B 744
ADP-2-10
MCL A 745
ADPQ-140-2
MCL B 744
ADP-2-10
MCL B 744
ADP-2-10
MCL B 538
SCA-4-15
-75
MCL
QBA-12
071838
MCL
SBA-2-20
071640
MCL
BP2C
MCL
BP4C

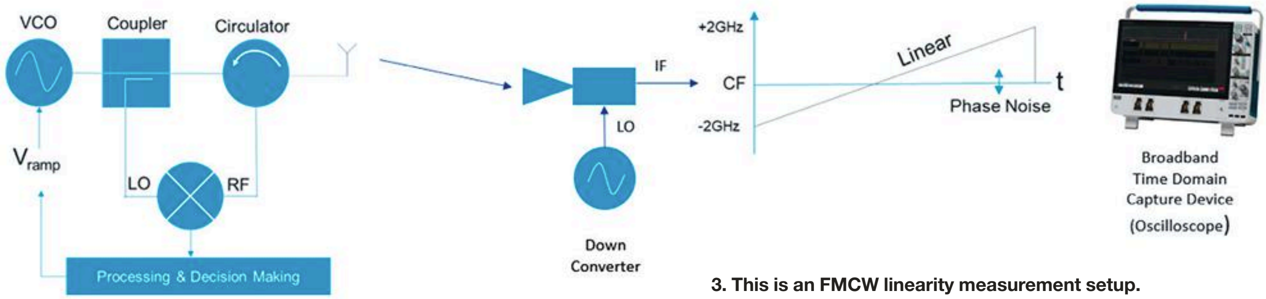

3. This is an FMCW linearity measurement setup.

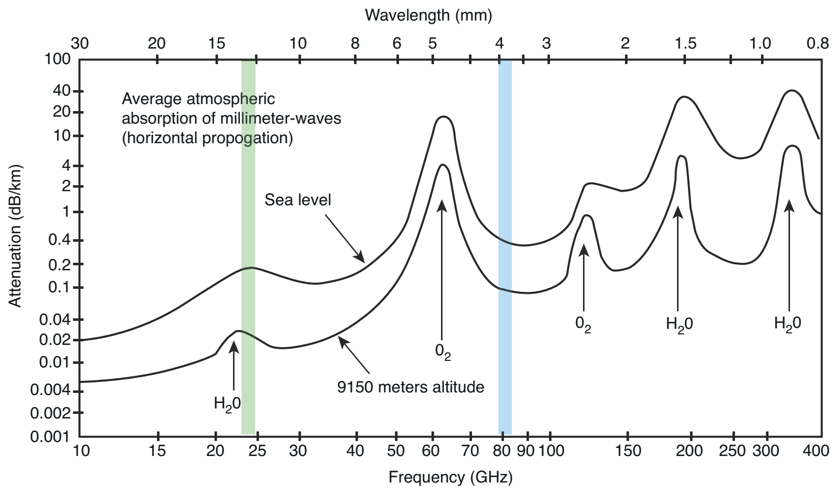

4. The green and blue bands indicate where there's potential for weather-related attenuation.

LINEARITY IS CRITICAL

The linearity of chirp waveforms is an important performance parameter of an FMCW radar. Any nonlinearity, or frequency distortion, will distort the measurement. As low-cost circuitry is often used in safety-critical and harsh environmental conditions, the linearity of the signal must be maintained.

Figure 3 shows the measurement of linearity being accomplished using a broadband time-domain capture device like an oscilloscope. The signal is downconverted from 76 or 81 GHz using a standard downconverter with a local oscillator to provide an IF frequency of around 5 GHz. The oscilloscope demodulates the FMCW modulation and then measures the linearity of the chirp.

When choosing a broadband acquisition device or oscilloscope, it's important to understand the performance of the instrument. In the example in *Figure 3*, the downconverter provides a 4-GHz signal that sweeps from 3 to 7 GHz. Therefore, an oscilloscope with at least 8 GHz of bandwidth or 25-Gsample/s sample rates and 8 bits of analog-to-digital converter (ADC) resolution is a good instrument. For chirps larger than 4 GHz, one may need a higher-frequency oscilloscope that can sample at 50 or 100 Gsamples/s.

The downconverter's performance is also an important consideration. Understanding harmonic performance is key. If, for example, one chooses a downconverter with a center frequency of 3 GHz, with a chirp bandwidth of 4 GHz, the harmonics of the 1.5-to-2.5 GHz signal sweep will fall in the measurement band.

Anyone who wants to look at the spectrum will also want to have a true spectrum analyzer on hand. Low-cost USB-based spectrum analyzers with an appropriate downconverter are very capable in terms of helping one understand the performance of the downconverter and ultimately the spectral performance of the automotive radar.

SIGNAL SIMULATION

Now that we've looked at the setup for signal analysis, let's take at what's involved with creating the signals to accurately simulate the real-world environment.

Although radar is largely immune to atmospheric conditions, it's important to be aware that at certain wavelengths or frequencies, the potential exists for attenuation either by oxygen molecules or water-vapor absorption. The green and blue lines in *Figure 4* show where the two bands lie (24/77 GHz). There's less atmospheric attenuation in the lower band and a bit more in the higher band. When developing LRR with a goal of obtaining maximum range, atmospheric conditions should be taken into account when testing the limits of a device.

Antenna performance is another variable. When designing the antenna system, the lobes should be kept as low as possible within the cost budget. Otherwise, false targets or clutter will be created. Various antenna patterns can be simulated with an arbitrary waveform generator (AWG). Targets also need to be recognized—not all objects are created equally.

When considering the well-known radar range equation, one of the elements is cross-section. Needless to say, the radar cross-section of a car can be very complex, involving a variety of materials with different absorption levels, such as metals, plastic, and composites. One also needs to consider multipath—how the radar behaves in a tunnel, for example.

Part of the qualification of any radar system involves testing a radar under a number of different target scenarios. It's another important factor that should be included in the signal simulation model built in the AWG. For radar millimeter-wave (mmWave) test applications, a capable AWG solution is needed. Among the critical requirements are:

5. A capable AWG is required to simulate the complex environment facing automotive radars.

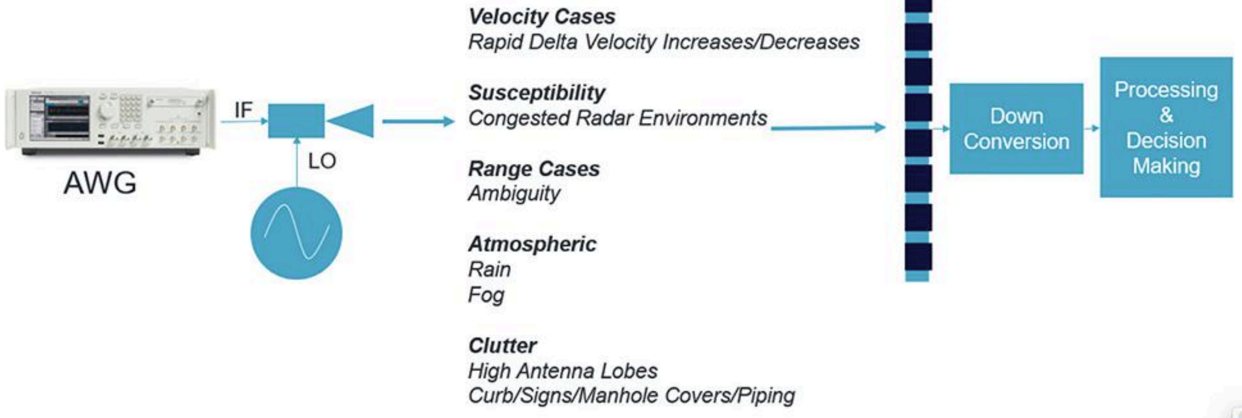

- Appropriate signal-generation software
- Frequency range up to 81 GHz
- Bandwidth of 4 GHz or more for high-resolution LFM
- Wide dynamic range to simulate antenna patterns and multiple target classifications
- Excellent frequency linearity
- Excellent phase noise—Doppler
- Phase control to emulate beamforming

In addition, it's often useful to be able to hook up multiple AWGs and perform different angle of arrival measurements, or to employ an AWG that has built-in multi-channel support.

The full-range scenarios that need to be created by an AWG for automotive radar are shown in *Figure 5*. Going down the list, we need to generate the radar cross-section and determine if an object is a car, truck, bike, or bridge street sign. Multiple velocity cases need to be emulated, such as a rapid change in velocity.

Of course, there will be other radars on the streets and it's only going to get more congested moving forward. Therefore, we need to test for susceptibility. Another challenge is range ambiguity: Are targets close together, far way, or all clustered together? Are atmospheric conditions reducing range? Finally, for LRR, clutter can be multiple objects such as curbs, signs, or even manhole covers. For SRR, all of these may be classified as targets.

CONCLUSION

Radar has been in use since WWII, so it's a tried and tested technology. With the recent move to 77 GHz, it looks well-positioned to play a significant ongoing role not only in ADAS, but also in the future of autonomous automobiles. Compared to the other sensors used in today's automotive applications, it has several advantages.

For example, cameras are susceptible to weather and darkness, passive infrared has temperature dependence, and laser/LiDAR is computationally intensive. Radar provides excellent range and velocity measurements, is immune to most weather conditions, works in the dark and over all temperatures, and is less computationally intensive than light-based sensor systems.

The move to 77 GHz offers significant improvements in range, resolution, and antenna size, but it does introduce new test challenges and requirements. Fortunately, modern test solutions like high-bandwidth oscilloscopes and high-performance AWGs give designers the tools they need to maximize radar performance under a wide range of conditions. mw

JEORGE S. HURTARTE | Product Marketing, LitePoint
MIDDLE WEN | Product Manager, LitePoint
www.litepoint.com

Over-the-Air Testing for 5G mmWave Devices: DFF or CATR?

This article investigates OTA test methods, such as direct far field and compact antenna test range, examining the tradeoffs in cost and path-loss performance.

With the advent of 5G millimeter-wave (mmWave) devices of various sizes and applications, each requiring different architectures and sizes of mmWave antennas, it's critical for test engineers to understand the differences in over-the-air (OTA) test chambers and test techniques. Direct far field (DFF) and compact antenna test range (CATR) are two types of OTA test methods supported by the 3GPP TR 38.810 Study on Test Methods for 5G FR2 (mmWave bands) devices.

Since CATR OTA chambers can cost up to 10 times more than DFF chambers, a test engineer must decide which one is best suited for the intended application and test requirements. Here, we will explain the differences between DFF and CATR chambers and the tradeoffs in cost and path-loss performance between the two types of chambers.

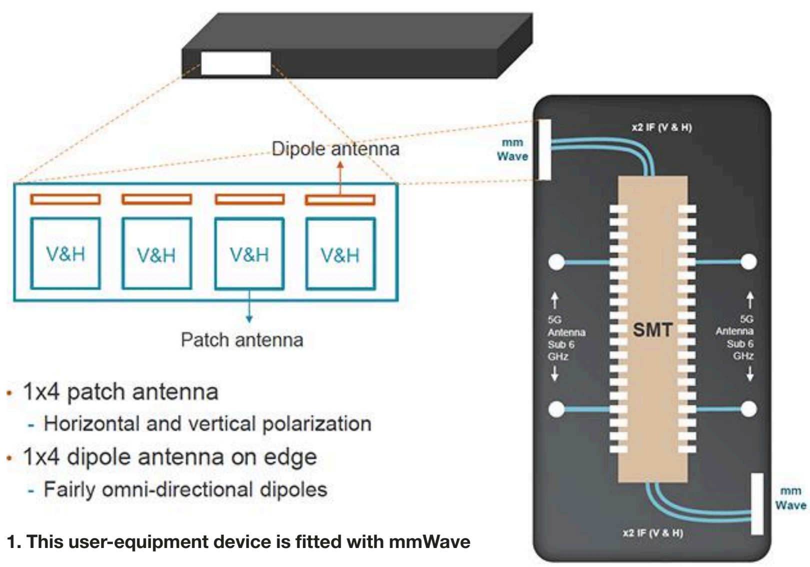

1. This user-equipment device is fitted with mmWave antennas.

INTRODUCTION

5G mmWave devices operating above 24 GHz incorporate millimeter-sized antenna arrays or dipole antennas, which become an integral part of the device module packaging. Thus, the only way to characterize and test the performance of the antennas as part of the final product is via OTA testing.

Figure 1 shows a user-equipment (UE) device (i.e., smartphone) with two built-in 5G mmWave modules, each containing a 1-×-4 patch antenna array and four dipole antennas. For this discussion, we will consider either the module or the final product as the device under test (DUT). For the example shown, each patch antenna element can have a vertical (V) or horizontal (H) polarization radiation pattern, which transmits or receives electromagnetic (EM) waves in either the vertical or horizontal direction.

When the antenna module is inside the final product, say, the smartphone, the antenna radiation pattern can be altered slightly due to the interaction with the final product enclosure materials and other surrounding components. Thus, the antenna performance, including its beamforming characteristics, needs to be tested using an appropriate OTA chamber of size, architecture, and shielding performance that ensures accurate antenna-radiation-pattern measurements.

5G mmWAVE OTA TEST METHODS

The 3GPP standards organization has published a technical document, TR 38.810, on 5G NR test methods.[1] It has declared that for UE RF test methods at mmWave frequencies, the following general aspects apply:

- OTA measurement is the testing methodology
- Permitted test methods are:
  1. DFF
  2. Indirect far field (IFF), also known as CATR
  3. Near-field to far-field transform

The test engineer's choice of the appropriate test method (DFF versus CATR, for example) has major implications in terms of capital equipment cost. CATR OTA chambers can cost as much as 10 times more than DFF OTA chambers. For all OTA test methods explained below, it's the responsibility of the UE manufacturers to "declare the antenna array size."

DIRECT-FAR-FIELD TEST METHOD

Typically, the exact locations of the antenna modules inside the UE DUT are well known. The DUT radiating antenna aperture dimension (D) is also known (expressed in cm). From this dimension, the required far-field distance (R) that separates the DUT from the test horn antenna can be derived using well-known mathematical equations, as explained later.

Per the TR 38.810 permitted test methods, if D ≤ 5 cm, the DFF test method can be used. This can translate to a significant OTA chamber capital cost savings. For example, a typical UE smartphone antenna module for UE smartphones, operating at both the 28- and 39-GHz frequency bands, has a D dimension of just below 3 cm—well within the "D ≤ 5 cm" requirement for the DFF chamber test method.

For DFF *(Fig. 2)*, the far-field distance (R) is the minimum distance at which the spherical waves can be considered as a "plane" wave at the receiving test antenna, thus fulfilling the following mathematical requirement:

$$R \geq \frac{2D^2}{\lambda}$$

where D is the diameter of the smallest sphere that encloses the radiating part of the DUT.

For D = 5 cm, the above equation yields a minimum far-field distance (R) of about 47 cm at 28 GHz. With the above equation, it can be shown that a 60-cm DFF OTA chamber, such as the one shown in *Figure 3*, satisfies the DFF test method requirements for a final product that has 5G antenna modules with apertures (D) of up to 4.5 cm at frequencies up to 44 GHz. Therefore, for existing 5G mmWave modules with D in the range of 3 cm, the DFF OTA chamber is the most economical choice.

3. A 60-cm DFF OTA chamber is shown with LitePoint's IQgig-5G mmWave tester.

INDIRECT-FAR-FIELD TEST METHOD

The IFF test method creates the far-field environment using a transformation with a parabolic reflector. This is also known as CATR.

Inside the CATR chamber, the DUT radiates a wave front to a range-antenna reflector that then collimates the radiated spherical wave front into a receiver-feed antenna *(Fig. 4)*. The separation between the DUT and the receiver is

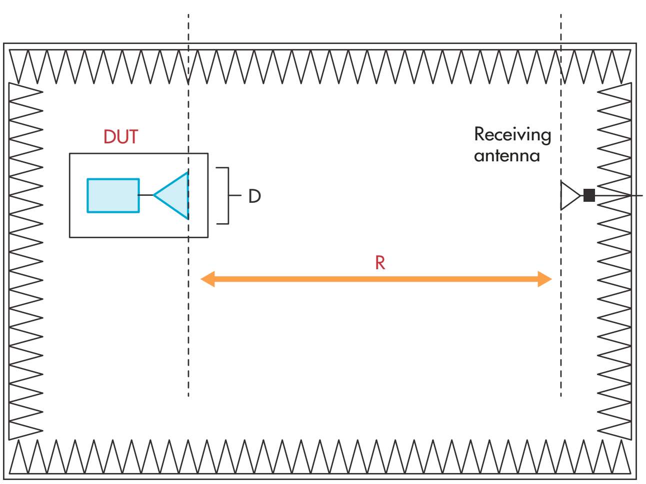

2. Here's a representation of a DFF OTA chamber (source Ref. 2).

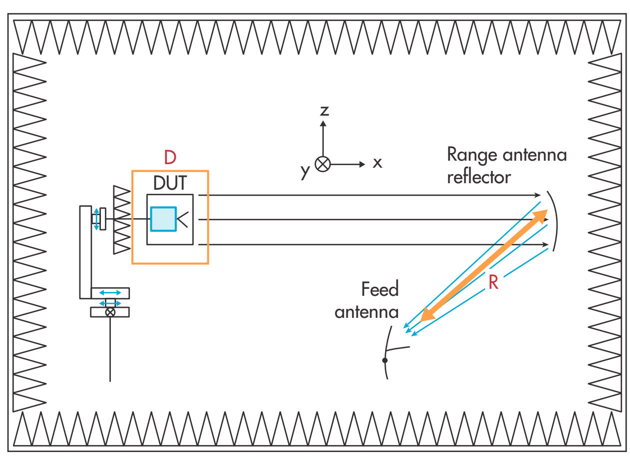

4. This drawing represents a CATR OTA chamber.

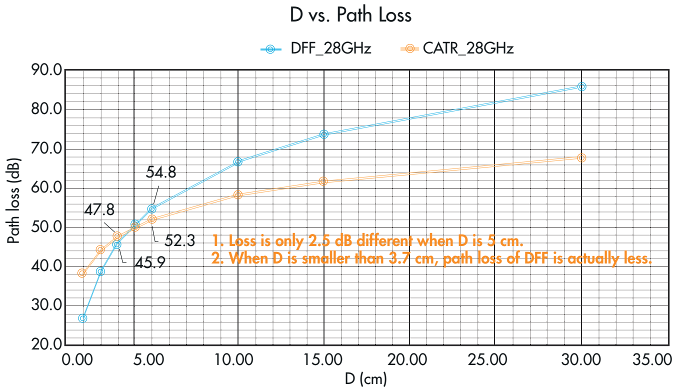

5. These plots compare DFF and CATR path loss at 28 GHz.

		28 GHz	39 GHz
DFF	D (cm)	2.78	2.78
	FF distance R (cm)	14.43	20.09
	Path loss (dB)	44.6	50.32
CATR	D (cm)	2.78	2.78
	Reflector size (cm)	5.56	5.56
	Focal length R (cm)	19.46	19.46
	Path loss (dB)	47.2	50.05

6. DFF and CATR path loss are compared at 28 and 39 GHz for D = 2.78 cm.

enough so that the emanating spherical wave reaches nearly plane phase fronts from transmitter to receiver.[2]

Per the 3GPP TR 38.810 document cited earlier, the CATR chamber test system does not require a measurement distance of:

$$R \geq \frac{2D^2}{\lambda}$$

to achieve a plane wave, as is the case with the DFF range. For CATR, the far-field distance (R) is seen as the focal length; that is, the distance between the "feed antenna" and the parabolic reflector. It's calculated using the following equation:

$$R = 3.5 \times \text{size of reflector} = 3.5 \times (2D)$$

For D = 5 cm, the CATR far-field distance, or focal length, is 3.5 × 2 × 5 = 35 cm, which allows for a more compact OTA chamber at the expense of a high-precision parabolic reflector.

NEAR-FIELD TO FAR-FIELD TRANSFORM TEST METHOD

The near-field to far-field transform test method computes the performance metrics defined for far field by using mathematical near-field to far-field transformations. Thus, the UE radiated near-field beam patterns are measured first. Next these measurements are translated into far-field metrics using the near-field to far-field mathematical transform.

Per TR 38.810, the near-field to far-field transform test method is only applicable for DUTs with radiating apertures of D ≤ 5 cm. A near-field to far-field transform test chamber can be smaller than DFF and CATR chambers, since the DUT is tested in the near field.

DFF VS. CATR OTA PATH-LOSS COMPARISON

As discussed in Ref. 3, OTA path losses can represent up to 94% of the total link budget in the OTA test setup. Thus, minimizing such path loss is of critical importance for the test engineer.

Figure 5 plots the path loss versus antenna aperture size (D) for both DFF and CATR OTA chambers. The path loss in dB is calculated using the Free Space Loss formula, with R = far-field distance:

$$\frac{\lambda^2}{(4\pi R)^2}$$

From *Figure 5,* at 28 GHz, the path loss is actually less for a DFF chamber when D ≤ 3.7 cm as compared with the path loss of a CATR chamber. As mentioned earlier, typical 5G UE antenna array modules have an aperture D in the range of 3 cm. Thus, the DFF OTA chamber is a better choice than the CATR OTA chamber in terms of path loss for D ≤ 3.7 cm.

Figure 6 compares the OTA path loss at 28 and 39 GHz for both DFF and CATR for D = 2.78 cm, the approximate dimension of a 1-×-4 antenna array for UE applications. As can be seen, the path loss of a DFF chamber is less than or equivalent to that of the CATR chamber at the same frequencies for the same DUT.

CONCLUSION

The choice of OTA test methods, DFF versus CATR for example, has significant implications on capital cost and path-loss performance. For UE DUTs that have built-in antenna arrays with D ≤ 3.7 cm in well-known locations inside the DUT, the DFF OTA test method yields capital-expenditure savings that are up to 10 times greater than the CATR method, with equivalent or lower path loss. mw

REFERENCES

1. 3GPP TR 38.810. 3rd Generation Partnership Project; Technical Specification Group Radio Access Network; NR; Study on test methods; (Release 16).

2. 3GPP TR 37.842. 3rd Generation Partnership Project; Technical Specification Group Radio Access Network; Evolved Universal Terrestrial Radio Access (E-UTRA) and Universal Terrestrial Radio Access (UTRA; Radio Frequency (RF) requirement background for Active Antenna System (AAS) Base Station (BS; Release 13).

3. Link-budget calculations: Needed for 5G OTA testing. Jeorge Hurtarte - January 22, 2019.

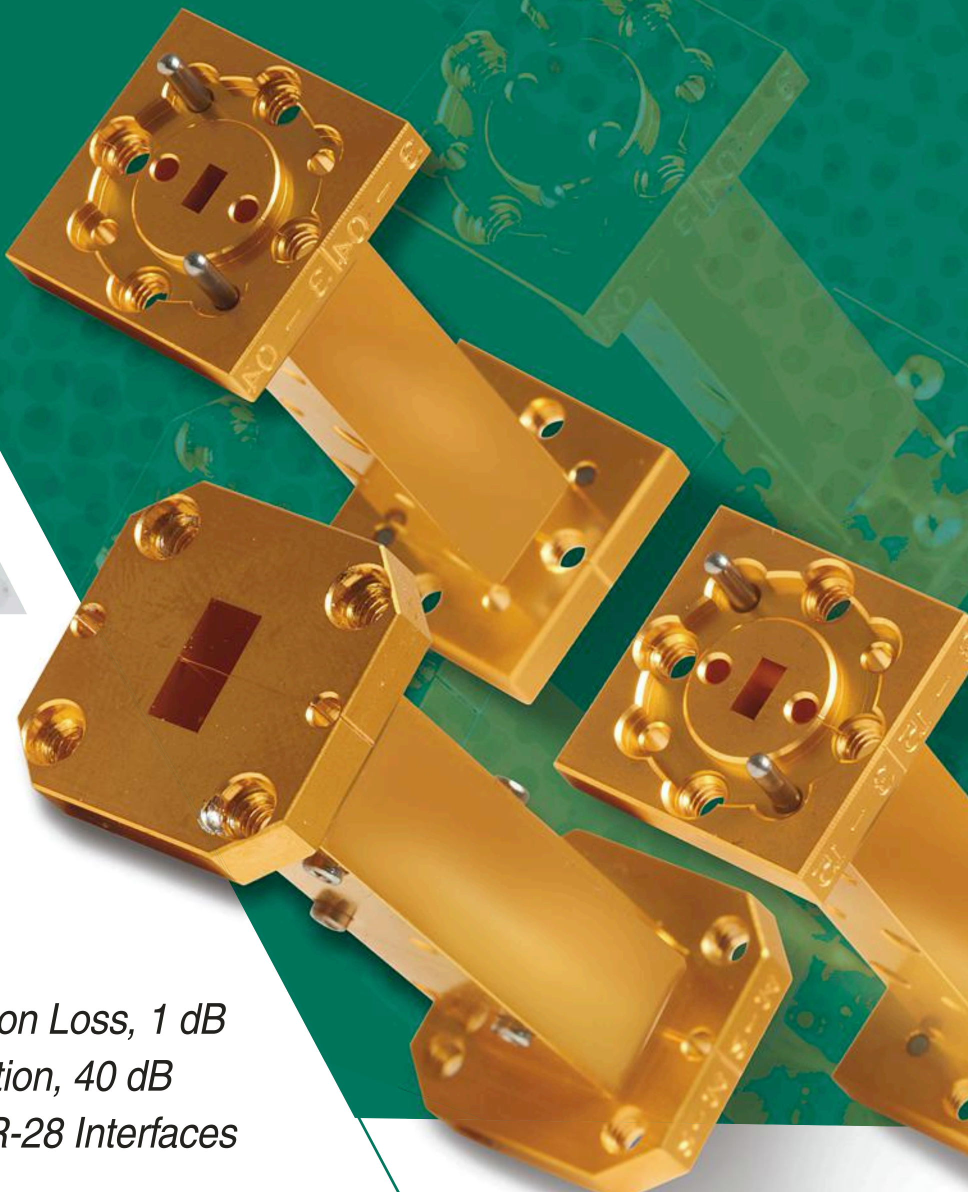

CHRIS DeMARTINO | Technical Engineering Editor

PEAK POWER SENSORS Offer More Than Meets the Eye

We take a firsthand look at a series of peak power sensors that demonstrate capabilities extending beyond basic power measurements.

1. The RTP5000 sensors can perform 100,000 measurements per second.

Power sensors are a specialty of Boonton Electronics *(www.boonton.com)*, which has a significant presence in the RF power-measurement world. The company's CPS2000 Series of true average connected power sensors was featured in an article last October titled, "Average Power Sensors Don't Settle for Average Performance." This article continues that theme by presenting a firsthand look at Boonton's RTP5000 Series of real-time peak power sensors *(Fig. 1)*. Boonton Electronics is a subsidiary of Wireless Telecom Group *(www.wirelesstelecomgroup.com)*.

A RUNDOWN OF THE RTP5000 SERIES

The RTP5000 Series consists of five models: the RTP5006, RTP5318, RTP5340, RTP5518, and RTP5540. The RTP5006 operates from 50 MHz to 6 GHz; the RTP5318 and RTP5518 from 50 MHz to 18 GHz; and the RTP5340 and RTP5540 from 50 MHz to 40 GHz. The sensors are used together with the Boonton Power Analyzer software that's downloadable from Boonton's website. Once the software is downloaded, simply connect the sensor to the PC with a USB cable to begin.

The RTP5000 sensors feature Boonton's Real-Time Power Processing (RTPP) technology. The company asserts that this technology enables the sensors to "capture, display, and measure every pulse, glitch, and detail with no gaps in data and zero latency." Another aspect of these sensors that Boonton likes to emphasize is the 195-MHz video bandwidth and the capability to measure rise times down to 3 ns. The company says the 195-MHz video bandwidth is "six times greater than what alternative products achieve." Therefore, according to Boonton, a video bandwidth in excess of 100 MHz makes the RTP5000 Series ideal for Wi-Fi and 5G signal characterization.

The RTP5000 sensors have a variety of use cases. Walt Strickler, VP/general manager at Wireless Telecom Group, says, "The main applications for the RTP5000 Series are characterization and design validation for commercial and military/aerospace radar, electronic warfare, and wireless communications (LTE, 5G, Wi-Fi)."

AN UP-CLOSE LOOK

Now, let's dive deeper into the RTP5000 Series by demonstrating some actual measurements using two RTP5006 sensors. To get a basic feel for the sensors and the Boonton Power Analyzer software, let's begin by showing a simple measurement of a pulsed-RF signal. In this example, a 2-GHz pulsed-RF signal will be measured with an RTP5006 sensor. The signal has a pulse width of 2 µs and a period of 10 µs.

Figure 2 reveals a trace measurement of the 2-GHz pulsed-RF signal using the Boonton Power Analyzer software. One significant aspect is the *Automatic Measurements* feature, shown on the left of *Figure 2*. This feature provides users with instant access to 16 different measurements, including pulse width, rise time, fall time, period, pulse repetition frequency (PRF), duty cycle, and more.

Furthermore, it should come as no surprise that the software allows users to specify many of the measurement settings. For example, by clicking the *Time/Trig* tab, one can set the timebase, trigger delay, and trigger position. Users also are able to set the trigger source, trigger mode, trigger level, slope (positive or negative), and holdoff.

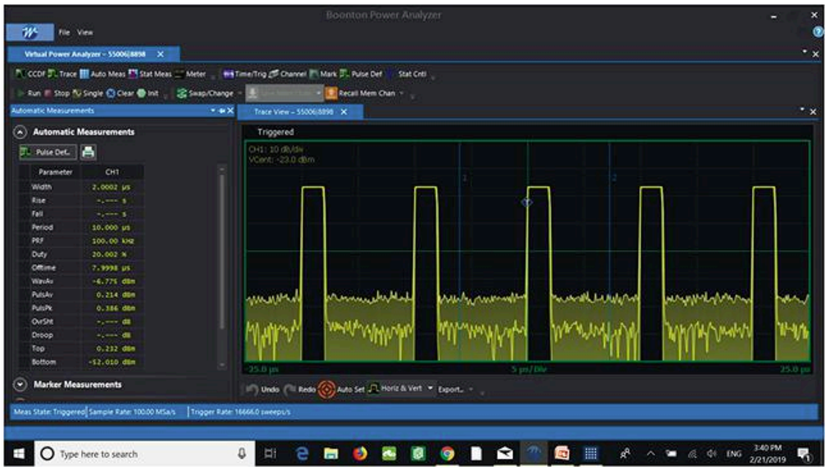

2. Shown is a measurement of a 2-GHz pulsed RF signal.

3. The demo aid is equipped with two output ports: *REF OUT* and *AMP OUT*.

GAIN AND PAPR MEASUREMENTS

Now that we've shown a very basic measurement, let's move on to something a little more advanced. A Boonton demo aid will be employed for the following measurement example *(Fig. 3)*.

The demo aid is quite a versatile box. Not only does it generate a signal, but also Gaussian noise. The noise can be used to effectively modulate the signal by toggling a switch on the front of the box.

The generated signal (with or without modulation applied by the noise source) then passes through a variable attenuator before being amplified by a 14-dB gain amplifier. The *REF OUT* port on the demo aid provides a reference of the generated signal before being amplified, while the amplified signal is provided through the *AMP OUT* port. Furthermore, the attenuation level can be adjusted using two dials.

When utilizing two sensors, it's possible to perform measurements like gain and propagation delay. Here, we'll look at a gain measurement. The demo aid will be used to generate a pulsed signal with a variable pulse width. An orthogonal-frequency-division-multiplexing (OFDM) signal can be replicated by modulating the pulsed signal with the noise source.

Two RTP5006 sensors will be used for this example. One of them is connected to the *REF OUT* port on the demo aid, while the other is connected to the *AMP OUT* port. The measure-

The RTP5000 Series consists of five models: the RTP5006, RTP5318, RTP5340, RTP5518, and RTP5540. The RTP5006 operates from 50 MHz to 6 GHz; the RTP5318 and RTP5518 from 50 MHz to 18 GHz; and the RTP5340 and RTP5540 from 50 MHz to 40 GHz. The sensors are used together with the Boonton Power Analyzer software that's downloadable from Boonton's website. Once the software is downloaded, simply connect the sensor to the PC with a USB cable to begin.

ments are synchronized by connecting a cable from the *MULTI I/O* connector of one sensor to the same connector of the other. This *MULTI I/O* connector serves as a trigger synchronization interconnect when multiple sensors are employed.

Figure 4 shows the trace measurement, with the pre-amplified measurement shown in yellow and the post-amplified measurement shown in blue. It should also be noted that the attenuation level of the demo aid was set to 10 dB.

After lowering the timebase to 5 µs/div, the markers can be placed in appropriate positions within the pulse for analysis *(Fig. 5)*. The *Marker Measurements* display, shown on the left, reveals that the average power over the marker interval (denoted as *MkAvg*) of the pre-amplified measurement is –11.169 dBm. The average power over the marker interval of the post-amplified measurement is +2.814 dBm, revealing a gain of about 14 dB as expected.

With the markers remaining where they are, a complementary cumulative distribution function (CCDF) analysis can be carried out by clicking the *CCDF* tab. A CCDF analysis is an effective way to examine peak-to-average-power-ratio (PAPR). A CCDF curve shows the time that the signal spends at or above a given power level.[1] The x-axis indicates how much the peak power exceeds the average power. The y-axis represents the percentage of time that the signal spends at or above the power level specified by the x-axis.

Figure 6 illustrates both pre-amplifier (yellow) and post-amplifier (blue) CCDF curves along with a Gaussian reference shown in grey. It reveals that the two CCDF curves are pretty closely aligned.

Now, let's change the attenuation to 0 dB. *Figure 7* shows the resulting CCDF curves. The post-amplifier (blue) CCDF curve is dramatically shifted to the left, revealing a significant amount of com-

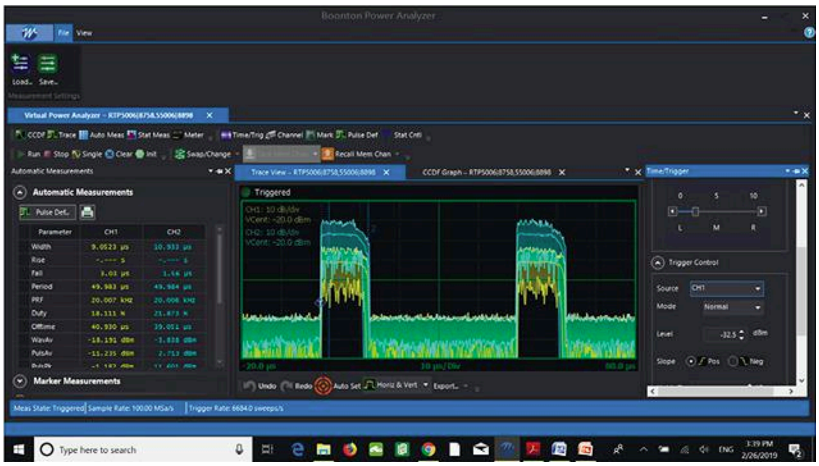

4. Pre-amplified and post-amplified measurements are shown in yellow and blue, respectively.

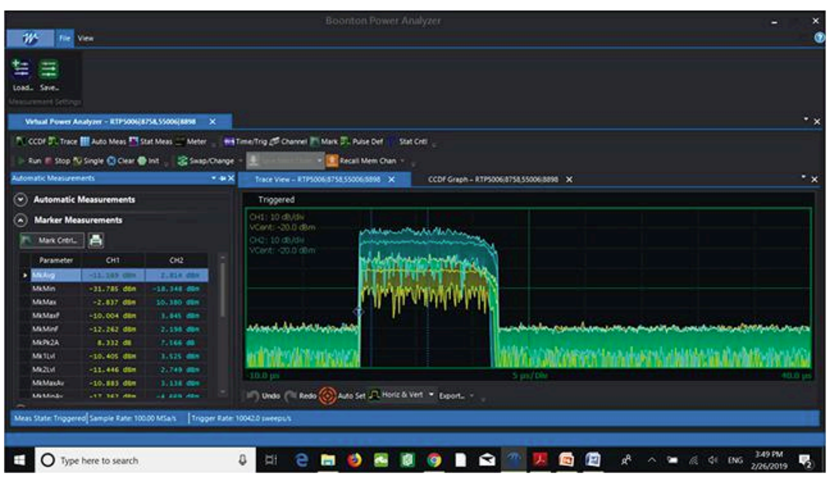

5. With the timebase set to 5 µs/div, the markers are placed within the pulse to measure gain.

pression due to lowering the attenuation (i.e., driving the amplifier harder). What this measurement demonstrates is that the RTP5000 sensors are a good tool for PAPR analysis.

CONCLUSION

The RTP5000 sensors offer capabilities beyond just simple power measurements, such as PAPR analysis, which was highlighted in this article. And while propagation-delay measurements were not presented, they are also possible thanks to the trigger stability of the RTP5000 sensors. Furthermore, while the software may take a little bit of time to get accustomed to, users should be able grasp it relatively quickly. To sum it all up, it looks like Boonton has a winning product line with the RTP5000 Series. mw

REFERENCE

1. Empower RF Systems, Using CCDF as a Method of Measuring P1dB and P3dB, Engineering Note.

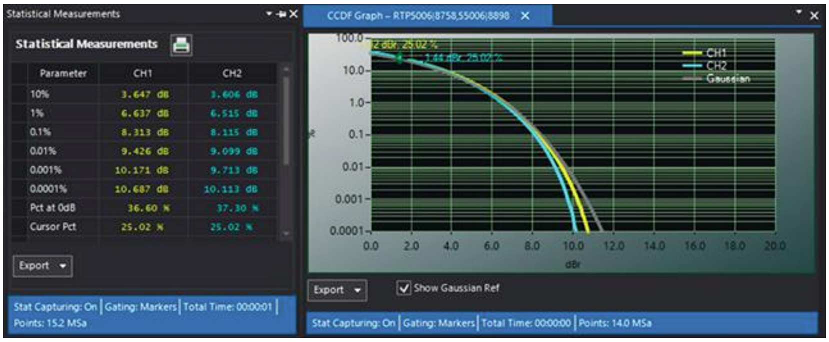

6. CCDF curves allow for a PAPR analysis.

7. The results here reveal compression due to setting the attenuation to 0 dB.

JEFF KAHLER | Technical Director, Nuhertz Technologies
www.nuhertz.com

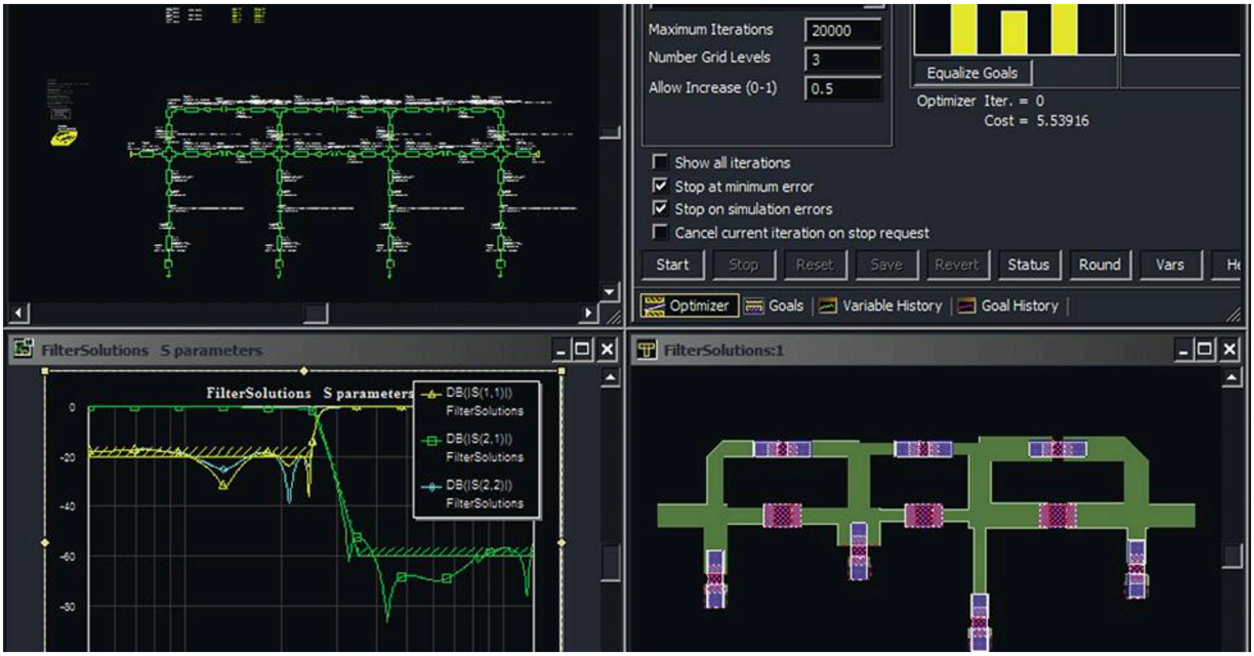

Complete Filter Design with Discrete Elements Made Easy

Features like internal part libraries and accurate models can greatly benefit anyone tasked with designing filters with discrete elements.

In an era of a myriad of design tools developed to "save" the filter designer time and effort, it's exactly time and effort that may be lost due to learning curves, cumbersome workflows, and limitations of the design process itself. Powerful design tools may thus be rendered effectively useless by any one of these problems.

For example, a tool that provides powerful synthesis may fall short when the output fails to be in a realizable form, or when users find the design process too cumbersome to waste time on. Furthermore, at higher frequencies, parasitic effects become increasingly difficult to manage, and countless hours may be wasted in the hardware lab if inadequate software is used.

Fortunately, design tools do exist that overcome these limitations. Specifically, Nuhertz Technologies offers FilterSolutions, which applies the best-suited manufacturer or internal parts model automatically selected from a user-customizable database, such as the NI AWR *(www.awrcorp.com)* software device library, Dassault Systèmes' *(www.3ds.com)* CST Studio Suite device library, or the Modelithics (*www.modelithics.com)* CLR Library within the NI AWR Design Environment platform.

For user-customizable libraries, users merely need to select a parts family, which may be custom built or supplied by the manufacturer(s). FilterSolutions then completes the design

process. In the case of higher frequencies (typically above 200 MHz), FilterSolutions exports directly into the NI AWR or CST Studio Suite design environments for interconnect simulations and further optimizations. Accurate lumped-element designs at very high frequencies may be quickly realized when using FilterSolutions with the NI AWR software and Modelithics. With the CST Studio Suite, other 3D features like the enclosure and connectors could be further added to the model.

INTERNAL PART LIBRARIES

For low-frequency designs (typically below 200 MHz), automated part selection generally involves just simply selecting the part family from a directory of S-parameter and/or Spice model libraries supplied by the manufacturers and/or created by the user. Nuhertz's patent-pending process employs easy-to-use pop-up menus of part families that make the learning curve negligible, enabling new users to quickly create accurate lumped designs with discrete parts.

Interconnect parasitics may be neglected initially, while the design accuracy is achieved by selecting a parts family with traits suitable for the design environment. Individual elements may be adjusted via a left-mouse click to individually select part families or S-parameter or Spice model files of specific parts *(Fig. 1)*.

COILCRAFT FILTER DESIGNER

For simple low-order Elliptic filters, Coilcraft's *(www.coilcraft.com)* Filter Designer offers discrete-inductor-element designs from Coilcraft libraries. It's freely available from the Coilcraft website. Coilcraft inductor samples may be obtained directly from the results screen.

NI AWR AND CST STUDIO SUITE SOFTWARE LIBRARIES

Users can directly export lumped filters designed with discrete elements from user libraries into NI AWR or CST Studio Suite. In addition, those using these Nuhertz partner tools may take advantage of the respective device libraries for high-frequency discrete-lumped-filter design. Use of the NI AWR Design Environment platform, specifically the Microwave Office software and the AWR website or MWO Vendor Local libraries, and the CST Studio Suite device library, is highly advantageous due to accurate and high-frequency simulation capabilities provided by microstrip interconnects. Interconnect geometry may be further optimized to achieve a closer match to design requirements.

Similar easy-to-use pop-up menus in the FilterSolutions export panel allow for selection of NI AWR, CST Studio Suite, or part family. FilterSolutions then exports the model that most closely matches the design value into the NI AWR or CST Studio Suite software, which is where the optimization goals are set up to enable the user to quickly optimize interconnect geometry as needed.

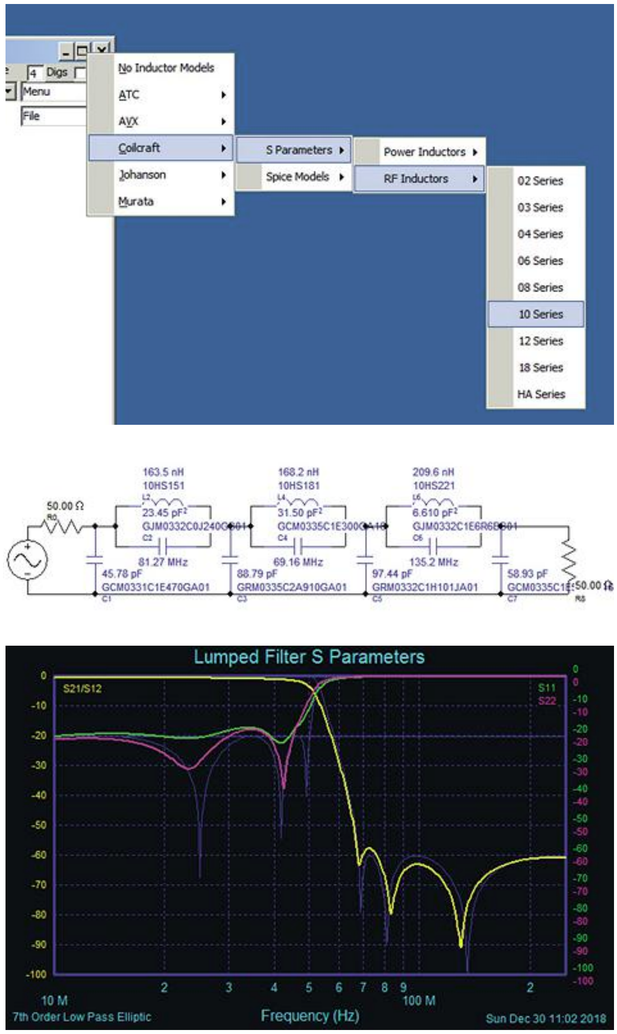

1. This is a 7-pole Elliptic example with Coilcraft 1008 Series S-parameter inductors and Murata 0603 temperature-compensating Spice model capacitors.

Furthermore, high-frequency lumped designs that require electromagnetic (EM) simulations for accuracy may be exported directly into NI AWR software, specifically the AXIEM 3D planar EM simulator or any of the NI AWR software partner EM simulators. These designs can also be exported into the CST Studio Suite software, where the 3D packages can be specified for the full-wave simulation model.

Optimization goals may be easily adjusted as needed in NI AWR and CST Studio Suite to obtain desirable results. One way to manually compensate for interconnect parasitic effects at higher frequencies is to design at a slightly higher frequency than the design requirements. One can then adjust the optimization goals down to the desired design frequency to obtain a reasonably close match between the initially designed filter

The easiest and most accurate method to design filters with discrete lumped elements is to use the Modelithics CLR Library of accurate part-value and substrate-scalable models in the NI AWR Design Environment framework.

and the required design frequencies. In the NI AWR software, the FilterSolutions export panel may automate this down-frequency adjustment *(Fig. 2)*.

CST STUDIO SUITE FILTER DESIGNER 2D

In CST Studio Suite, Filter Designer 2D provides a seamless workflow for the design of lumped-element filters, with the underlying technology based on Nuhertz software. Once a filter is synthesized, the fully parameterized model is built in the CST Studio Suite schematic environment from which further analysis can be triggered. A 3D model is automatically configured by the System Assembly and Modeling, and it may include the package footprint of each lumped component. A range of full-wave EM solvers are available for either frequency- or time-domain analysis, while the optimizer can be setup with either S-parameter masks or the recently introduced coupling matrix extraction technique *(Fig. 3)*.

MODELITHICS LIBRARY IN NI AWR DESIGN ENVIRONMENT

The easiest and most accurate method to design filters with discrete lumped elements is to use the Modelithics CLR Library of accurate part-value and substrate-scalable models in the NI AWR Design Environment framework. Modelithics employs exceptional and highly scalable (and therefore tunable) modeling accuracy.

FilterSolutions takes advantage of the Modelithics/NI AWR software interface to set up discrete optimizers that very rapidly zero in on the best overall choice of Modelithics models for each lumped-filter element. It then sets the interconnect optimization flag in the NI AWR software so that the user can optimize the interconnect geometry. Accurate, discrete multigigahertz lumped-element filter designs may be realized very rapidly using Nuhertz together with Modelithics and the NI AWR Design Environment software.[1]

For higher-frequency designs (i.e., above 1 GHz), the AXIEM 3D planar EM simulator may be employed to analyze detailed EM effects. It may also be used for extraction optimization, if necessary *(Fig. 4)*. mw

REFERENCE

1. I. Delgado, L. Levesque, L. Dunleavy, and J. Kahler, "Synthesize Filters with Wideband Success," *Microwaves & RF*, July 2014.

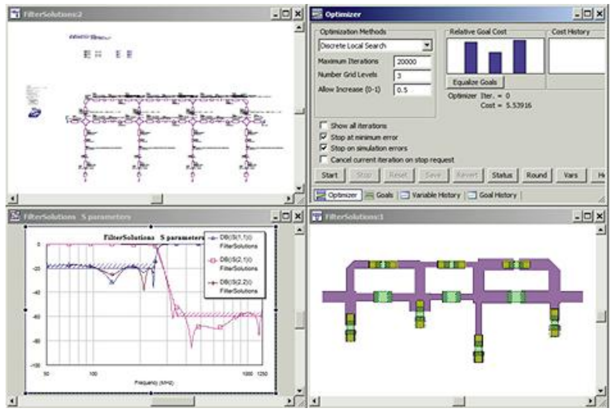

2. Shown is a 250-MHz and pole Elliptic discrete-filter design with the NI AWR software web library and Coilcraft 1008 Series inductors and AVX Accup-0603 capacitors.

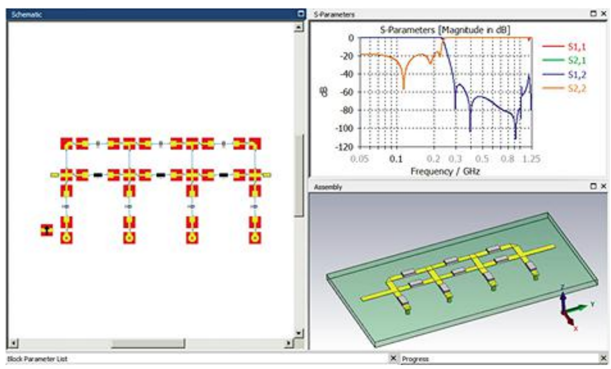

3. This screenshot depicts a 250-MHz 7-pole Elliptic discrete filter design in CST Studio Suite using the device library with Coilcraft 1008 Series inductors and TDK capacitors.

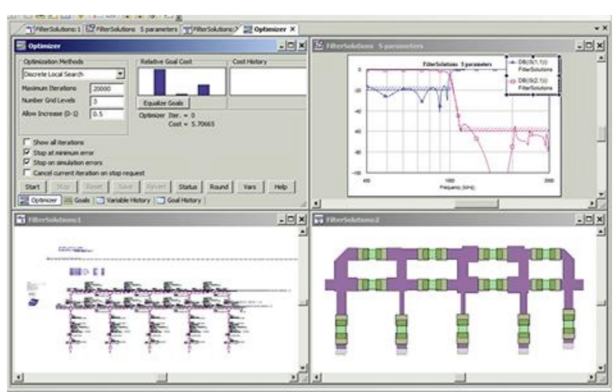

4. This is a 1-GHz, 9-pole Elliptic filter designed with discrete lumped elements using FilterSolutions with the Modelithics CLR Library models and NI AWR software.


HI-REL
SPACE QUALIFIED
PRODUCTS
Adelson Family Foundation
SPACEIL
Kahn Foundation
Nancy and Stephen Grand Fund
SYLVAN ADAMS
IAI
עם ישראל חי
Proud Sponsor of
SpaceIL Moon Mission
Mini-Circuits®
www.minicircuits.com
SPACEIL
597 RevOrig_INT

defense electronics

A Special Section to INFORMA'S DESIGN ENGINEERING & SOURCING GROUP MARCH 2019

NASA Selects Texas A&M to Test Drone Management

JACK BROWNE | Technical Contributor

NASA chose the Lone Star UAS Center of Excellence and Innovation at Texas A&M University-Corpus Christi as one of only two sites across the U.S. to test drone traffic management.

AS MORE DRONES take to the skies, safety has become a primary concern. To ensure that unmanned aerial vehicles (UAVs) do not interfere with both manned and unmanned vehicles of other kinds, NASA's Unmanned Aircraft Systems Traffic Management (UTM) project selected the Lone Star UAS Center of Excellence and Innovation *(www.lsuasc.edu)* at Texas A&M University-Corpus Christi as one of only two sites across the U.S. to test drone traffic management.

The Lone Star team plans to start testing this summer, focusing on drone communications, collision avoidance, safe landing, safety in urban environments, and services that support UAS operations. NASA's UTM project works closely with the Federal Aviation Administration to conduct field demonstrations of small unmanned aircraft systems to fully and safely access low-altitude airspace in support of civil and business opportunities.

"The Lone Star Team is proud to have been selected by NASA to work on such critical testing efforts," said Mike Sanders, Acting Executive Director of the Lone Star UAS Center of Excellence & Innovation. "This series of tests is a critical step in enabling the safe integration of unmanned aircraft systems within an urban environment. We look forward to working with NASA's Ames Research Center, the City of Corpus Christi and its first responders, the Corpus Christi International Airport, the Port of Corpus Christi, as well as the many partners across Texas and the United States."

(Continued on page 52)

SEWIP Block 2 is Key Player in U.S. Navy's Systems

THE U.S. NAVY depends on its electronic-warfare (EW) systems to keep pace with technology. One such system is the Surface Electronic Warfare Improvement Program (SEWIP) Block 2, which is an upgrade to existing AN/SLQ-32(V) EW systems. The latest improvements involve enhancements to receivers and antennas to achieve the sensitivity needed to track current threats even when immersed in noise. To maintain a technological edge, the Navy recently awarded Lockheed Martin a $184 million firm-fixed-price modification to exercise options for full-rate production of SEWIP Block 2 systems.

"We are honored to continue to provide this critical fleet defense capability that our warfighters rely on while they perform their mission worldwide," said Joe Ottaviano, Integrated Electronic Warfare program director, Rotary and Mission Systems. "Threats are changing and evolving faster with advanced technologies and the SEWIP system will give the U.S. Navy the advantage of remaining one step ahead of our adversaries."

(Continued on page 52)

How 5G Could Impact the Military

JACK BROWNE | Technical Contributor

COMMERCIAL MEDIA attention to 5G cellular wireless communications systems has grown steadily in recent months, in anticipation of a wireless communications network that will leave no stone unturned and possibly no citizen without a cellphone. But what does such a significant technological introduction as 5G, with its massive infrastructure building on top of existing 3G and 4G Long Term Evolution (LTE) towers, mean to defense electronic technology?

Military system designers, of course, will take advantage of available 5G hardware and software for current and future systems, benefiting from such features as fast response times and wide bandwidths that allow for, say, lightning-fast transmission and reception of images representing battlefield scenarios.

Perhaps the real question will be: Can all potential future 5G users coexist? Natural limiting factors for military communications systems, such as mountainous terrain and rainfall attenuation, will impact the effectiveness of 5G systems in all cases.

Achieving full performance of military 5G technologies with minimal interference from operating environments and other users will depend on creative computer software simulations. It will also require effective measurement strategies to predict the different operating scenarios that an almost "unlimited" number of 5G users, commercial and military, will face.

Military designers can take advantage of different, more ruggedized components and packaging than used in more cost-conscious commercial radios, and perhaps unique military nuances to the operating environment, such as portable, transportable 5G base stations that can be moved around as needed. But they will face the usual obstacles to overcome from opposing forces, such as high-power jamming signals.

Whether for military or commercial users, 5G wireless networks will depend on higher-frequency signals, such as 28 GHz and beyond, traveling shorter distances, compared to 4G networks that operate with longer-wavelength, lower-frequency signals. The consumption of bandwidth at lower frequencies has quickly limited the transmission speeds of 4G wireless networks to the Mb/s range. On the other hand, 5G system designers are hoping to reach transmission speeds of 1 Gb/s and beyond.

Military users will no doubt benefit from the available bandwidths and transmission speeds of 5G devices, along with the reduced lag times of those higher-frequency, millimeter-wave signals. As always, the problems will come from an adversary's use of the same wireless communications technologies, which will be freely available to all. de


NATIONAL INSTRUMENTS
TOMORROW'S DESIGNS REQUIRE
SMARTER
SOFTWARE TODAY
AWR
NI AWR Design Environment software provides a seamless platform for developing next-generation wireless electronics and communication systems, from concept to product. Its powerful interface, integrated system, circuit, and electromagnetic simulation technologies, and design flow automation ensures your design success.
Visit awrcorp.com/smarterdesign to learn more.
©2019 National Instruments. All rights reserved. AWR, AWR Design Environment, National Instruments, and NI are trademarks of National Instruments. Other product and company names listed are trademarks or trade names of their respective companies.

Texas A&M to Test Drone Management *(Continued from page 49)*

NASA *(www.nasa.gov)* has been involved in a series of drone technology testing, increasing the complexity of tests each year. "Our (program) represents the most complicated demonstration of advanced UAS operating in a demanding urban environment that will have been tested to date," said Ronald Johnson, NASA UTM project manager. "For the commercial drone industry to really advance, they need to see the results of this testing to understand the opportunities and challenges posed by flying in an environment where communications, GPS navigation, micro weather, tall buildings, and community acceptance all present hurdles to everyday, safe operation." de

SEWIP Block 2 is Key Player in U.S. Navy's Systems *(Continued from page 49)*

Under this full-rate production contract, Lockheed Martin will continue providing and upgrading the AN/SLQ-32 systems on U.S. aircraft carriers, cruisers, destroyers, and other warships. Lockheed Martin was awarded an initial $148.9 million contract in 2016 by the Navy for full-rate production of SEWIP Block 2 systems, with four additional option years to keep pace with evolving threats. The firm has supported the U.S. Navy with SEWIP Block 2 development, production, and engineering services since 2009. de

Lockheed Martin is upgrading AN/SLQ-32 systems on U.S. Navy vessels as part of a SEWIP Block 2 system contract.

COBHAM BACKS NATO WITH ANTI-SHIP MISSILE DEFENSE

COBHAM PLC *(www.cobham.com)* will be supplying electronic-warfare (EW) training pods to NATO for the Joint Electronic Warfare Core Staff (JEWCS) capability package, as part of a contract to Leonardo (www.leonardocompany.com). The company will deliver full Air and NATO Anti-Ship Missile Defence Evaluation Facility (NASMDEF) systems. Cobham's training pods provide EW training through radar and communications jamming as part of threat simulation. The JEWCS and NASMDEF systems enable NATO forces to remain ready to react to current and emerging threats.

Paul Armstrong, senior vice-president and general manager said, "We are delighted to have secured this contract which demonstrates Cobham's extensive experience delivering EW training and supporting pod technology. We have been developing our latest pods to meet the increasingly sophisticated, ever-changing and future threats faced in contested environments. Cobham is committed to working with Leonardo to provide NATO with the latest generation training and technology solutions to support effective operations with the electronic warfare environment." ■

Cobham will provide NASMDEF systems to Leonardo for the NATO JEWCS program. *(Courtesy of Cobham plc)*


65GHz
50GHz
40GHz
Mini-Circuits
Mini-Circuits
Mini-Circuits
Coaxial Adapters, Amplifiers, Attenuators,
Couplers, Splitters, Terminations & Test Cables
Breaking Through Barriers to the Next Generation of Wireless Applications
Mini-Circuits®
www.minicircuits.com P.O. Box 350166, Brooklyn, NY 11235-0003 (718) 934-4500 sales@minicircuits.com 566 Rev F

Government "Rodeo" Demonstrates Tank Protection Against ATGMs

NORTHROP GRUMMAN CORP. *(www.northrop-grumman.com)* recently demonstrated the effectiveness of its vehicle-protection technologies against advanced anti-tank guided munitions (ATGM) systems during a U.S. government-sponsored soft-kill "rodeo" late last year in Huntsville, Ala. Northrop's Vehicle Active Protection System was deployed onboard an M1A1 Abrams tank *(see figure)* on a live-fire range during a month-long demonstration of testing soft-kill capability against real-world threats, including ATGM systems. The demonstrations were sponsored by the U.S. Army Tank Automotive Research Development Engineering Center (TARDEC).

An M1A1 Abrams tank was used to demonstrate the effectiveness of Northrop Grumman's vehicle-protection technologies against real-world threats. *(Courtesy of Northrop Grumman)*

During the demo, Northrop Grumman used its passive-infrared (IR) cueing sensors system to issue threat warnings of inbound ATGMs, providing a cue for the tank's onboard soft-kill countermeasures (SKCM) system. The protection system, known as the multifunction electro-optical system (MEOS), countered the ATGM and defeated it in real time. The MEOS, an adaption of airborne-system protection technology, identified and countered all types of threats fired at its APS system.

"This solution is an example of leveraging significant investment in aircraft protection to rapidly provide similar capabilities to ground vehicles," said Mike Meaney, vice president, advanced missions, Northrop Grumman. "We look forward to working with the Army to deploy an affordable end-to-end Vehicle APS system that can defeat a variety of anti-tank guided munitions." ■

Flight Data Recorders Receive ETSO Approval

CURTISS-WRIGHT'S Defense Solutions division was granted European Technical Standard Order (ETSO) approval by the European Aviation Safety Agency (EASA) for its Fortress family of flight data recorders (FDRs). This family of "black boxes" includes cockpit data recorders (CDRs), datalink recorders (DLRs), airborne image recorders (AIRs), and FDRs that surpass minimum EASA 2021 requirements of 25 h recording time. In addition, these FDRs feature a modular architecture that can be readily adapted to changing performance and applications requirements.

The Fortress FDRs are the first such recorders to meet the requirements of EUROCAE ED-112A, allowing aircraft data to be used for more efficient operations. EASA certifications include ETSO-C123c, ETSO-C124c, ETSO-C176a and ETSO-C177a.

"We are excited to announce that our Fortress family of recorders, the most advanced lightweight and functional flight recorder available today, has been granted ETSO approval," said Lynn Bamford, senior vice president and general manager, Defense Solutions div. "We are the first supplier to meet flight recorder extended operational requirements and increased crash survivability test requirements included in ED-112A, furthering our commitment to helping aircraft meet the latest regulations while using the best technology to add more functionality in less space and cost for new and older aircraft." ■

The Fortress family of FDRs includes compact, modular units with multiple recording functions. *(Courtesy of Curtiss-Wright)*

JACK BROWNE | Technical Contributor

How to Select the Right Data Converters

Versatile and power-efficient data conversion is a part of defense systems, from audio through microwave frequencies, and choosing the right data converters means weighing several key performance parameters.

DATA IS essential to any military defense system, and handling data efficiently usually is the task of a handful of key components. But perhaps no components are more important in an advanced signal-processing system than its analog-to-digital converters (ADCs) and digital-to-analog converters (DACs), which cannot afford to fail or even be slightly in error.

Suppliers of ADCs and DACs have made impressive advances regarding processing power for power consumed in these components over recent years, and troops around the world (and sometimes in space) rely heavily on the performance of these components in stationary and portable systems. Often, finding the right data converter for a system design is simply a matter of understanding the relevance of different data-converter specifications and which of those are the most important for an application.

ADCs and DACs are typically used in systems with signal amplifiers, filters, digital signal processors (DSPs), and other components to help with the extraction of information from processed signals. Typically, data converters are specified first in a system design, setting the performance limits for that system (and the requirements for many of the system's other components). By placing the ADCs as close to the antennas as possible, for example, the antenna's dynamic and frequency ranges can be digitized quickly by the ADCs for analysis in the digital realm.

Many defense-based systems are designed for portability, such as software-defined radios (SDRs), for applications driven by designs that require minimal power consumption for extended operating periods on battery power. The rechargeable battery is part of the portability and must be as small and light in weight as possible while still providing the energy requirements of an SDR's various components, including ADCs and DACs.

SAMPLING ADCs

One fundamental requirement when choosing an ADC is determined by the frequency of the analog input signal to be processed. According to Nyquist sampling theory, the signal to be digitized should be sampled at a speed that's more than two times the analog frequency, with higher sampling rates providing greater details about the signal to be sampled. Those higher sampling rates usually come with higher ADC power requirements, however, resulting in the need to weigh a set of data-converter

1. Model AD4020 is an example of a high-resolution ADC, at 20 bits. It samples analog input signals at 1.8 Msamples/s, but only consumes 15 mW from a +1.8-V dc supply at the maximum sampling rate. *(Courtesy of Analog Devices)*

2. To save power and size, ADCs such as the model LTC2358-18 from Linear Technology/Analog Devices pack eight channels, each with its own ADC, within a miniature package that has many supporting components. *(Courtesy of Analog Devices)*

3. When moving from digital code back to analog signals, converters such as the AD5766 and AD5767 denseDACs provide 16 channels of processing with high resolution by means of 16 separate DACs within a small package. *(Courtesy of Analog Devices)*

Selecting an ADC for any system application is a matter of weighing the different ADC performance parameters versus the requirements of the application, such as power consumption in a portable radio and a high sampling rate for a high-frequency application. The bit resolution of an ADC can be critical to some applications, such as for a radar onboard a ship or aircraft that must be capable of discerning a small weapon (e.g., a missile) against a much larger background.

performance parameters when trying to also achieve extended operating times on battery power.

Nyquist theory is based on sampling repeatable signals, such as sinewaves without deviations or modulation. The more irregularities in the signal to be sampled, the greater the need for an ADC with a higher sampling rate to capture any deviations in the signal flow. Additional components, such as anti-aliasing filters, can help achieve effective digitization of input signals when the available ADC sampling rate may be considered low for the signals to be sampled.

Selecting an ADC for any system application is a matter of weighing the different ADC performance parameters versus the requirements of the application, such as power consumption in a portable radio and a high sampling rate for a high-frequency application. The bit resolution of an ADC can be critical to some applications, such as for a radar onboard a ship or aircraft that must be capable of discerning a small weapon (e.g., a missile) against a much larger background.

Higher bit resolution will be needed to separate irregularities in processed pulses, such as the delays and amplitudes of pulses reflected from a jet aircraft compared to the pulses returning to a radar receiver from a jet-fired missile. As with many other ADC performance parameters, though, high-resolution ADCs like 20-b converters typically provide much lower sampling rates than that available with lower-resolution ADCs, such as 8-b converters.

When comparing different model ADCs from Texas Instruments *(www.ti.com)*, for example, greater bit resolution means lower sampling-rate speeds. For a bit resolution of 16 b, for example, the highest-speed ADC operates at 200 Msamples/s. For slightly less bit resolution of 14 b, the firm's best ADC operates at a top sampling rate of 400 Msamples/s. This trend of decreasing bit resolution for increasing sampling rate follows for other TI ADCs, with a 12-b ADC providing up to 2-Gsample/s rates and its fastest 8-b ADC operating at 3-Gsample/s or better sampling rates.

These ADCs are typical of the trends found in bit resolution versus sampling rates. In addition, higher numbers for both specifications usually mean higher power consumption for an ADC compared to a component with lower bit resolution and sampling rates.

For many systems, noise performance is important; an ADC's datasheet will provide information on a converter's signal-to-noise ratio (SNR) and its total harmonic distortion (THD). High values indicate a converter that can detect small or weak signals in the presence of interfering signals and/or noise, transforming input signals into meaningful code for processing by the other components in the system, such as DACs and digital signal processors (DSPs).

Aperture jitter or uncertainty is another ADC noise parameter, a measure of the sample-to-sample variations in aperture delay, typically measured in piscoseconds root mean square (RMS). It may appear as frequency-dependent noise on an ADC's input port and can convert to phase noise within a system; thus, it should be minimized.

Many converter suppliers, including Analog Devices *(www.analog.com),* have developed functions and features to conserve ADC power. High-resolution ADCs such as the 20-b AD4020 *(Fig. 1)* are designed to save power where possible; for example, using fully differential input ports and a high-impedance mode so that the ADC can be driven directly with lower-power precision amplifiers. The ADC also operates with a low serial peripheral interface (SPI) clock-rate requirement for reduced power consumption. The AD4020 runs from a +1.8-V dc supply and achieves relatively high processing speeds, at 1.8 Msamples/s, but only consumes 15 mW power at its maximum rated sampling speed and less power at lower sampling speeds.

The model LTC2358-18 from Linear Technology, now part of Analog Devices *(Fig. 2)*, simultaneously samples on eight channels with as much as 200-ksample/s throughput per channel. It has differential inputs and an internal clock to minimize latency in the sampling cycles and guarantees 18-b resolution, with no missing codes.

In terms of functionality, the LTC2358-18 is an example of a densely packed device well-suited to the audio range. Replete with an integrated reference source and buffer amplifier, it's capable of a typical 96.4-dB single-conversion SNR. When working with audio signals, the ADC features THD of typically −111 dB for a 2-kHz input signal. It includes SPI CMOS and LVDS serial input/output (I/O) interfaces for ease of control interconnections, using a 7- × 7-mm LQFP package with 48 leads for connections to the SPI CMOS and LVDS serial interfaces.

RETURN TO ANALOG

On the other side of the system, DACs provide the reverse functionality of an ADC to return digital representations of signals to analog form. For most receivers, a set of DACs will provide almost "mirror-image" functionality and performance to that of its ADC cousins, converting code with the same bit resolution and sampling rates. For instance, the tradeoffs in power consumption and performance typical of ADCs are also present for DACs and should be weighed against system requirements as well as for compatibility with the ADCs in a system. Depending on the system design, DACs can provide low- or high-voltage outputs, with single-voltage outputs for simpler designs, multiplying outputs for higher-frequency configurations, and current-output devices when required.

As an example, the AD5766 and AD5767 denseDACs from Analog Devices are 16-channel, 16- and 12-bit DACs that are highly integrated with supporting components, including reference buffer amplifiers, multiplexers, and channel-monitoring multiplexers *(Fig. 3)*. Incorporating 16 independent DACs within each package, they are compatible with 1.8-V logic and generate analog output voltages from an external 2.5-V reference.

Both devices are available within either of two compact housings: a 4- × 4-mm, 48-lead WLCSP and a 6- × 6-mm 40-lead LFCSP. The DACs feature eight software-programmable output ranges, including −20 to 0 V, −16 to +10 V, and ±5 and ±10 V, and integrated DAC output buffers capable of ±20 mA current. The operating temperature ranges for both DACs is −40 to +105°C.

This brief rundown of some readily available ADCs and DACs provides a "sampling" of how the specifications change depending on specific requirements. For example, higher resolution is available for lower frequencies, along with impressive integration of multiple components to achieve many channels within a multipin or multiple-lead surface-mount-technology (SMT) package. While no single ADC or DAC provides the ultimate performance levels that can satisfy all system requirements, smart selections can be made by using the most critical requirements of a system, such as size, power, or resolution, to help guide the choice. de

JACK BROWNE | Technical Contributor

AWGs Pack More Memory at Rates to 50 Gsamples/s

These high-performance single- and dual-channel arbitrary waveform generators set new standards for DAC sampling rates and vertical resolution, producing RF/microwave outputs to 20 GHz.

SIGNAL GENERATION has never been more complex, given the many types of analog and digital signals blended in modern communications and radar systems. To keep pace with generating realistic signals for testing these systems, Tektronix developed the AWG70000B Series arbitrary waveform generators (AWGs), which can be equipped with as much as 32-Gsample waveform memory to operate at waveform sampling rates to 50 Gsamples/s.

Of course, all that digital-to-analog-conversion (DAC) firepower would be inconsequential without the precision of 10-bit vertical DAC resolution using DACs capable of –80 dBc spurious-free dynamic range (SFDR). AWGs incorporate one or more high-speed DACs per channel to generate complex output waveforms when the DACs are fed digital representations of signals from stored waveform libraries.

The AWG70000B Series arbitrary waveform generators (AWGs) include single-channel models capable of outputs to 20 GHz and dual-channel models with separate outputs each to 10 GHz.

THE AWG70000B SERIES AWGS		
	AWG70001B	AWG70002B
Channels	One	Two
Vertical resolution	10 bit	10 bit
Maximum sampling	50 Gsamples/s	50 Gsamples/s
Standard memory	2 Gsamples	2 Gsamples
Maximum memory	32 Gsamples	16 Gsamples/channel
Maximum frequency	20 GHz	10 GHz
SFDR	–80 dBc	–80 dBc
Minimum rise time	27 ps	22 ps

The Tektronix AWG70000B Series features the single-channel model AWG70001B and the two-channel model AWG70002B AWGs *(see figure)*. The single-channel source can generate output waveforms to 20 GHz, while the dual-channel source provides two separate outputs, each as high as 10 GHz in frequency. The high-speed AWGs each include a dedicated Ethernet streaming ID connector on the rear panel with Streaming Waveform ID functionality for connection to a PC.

By using these AWGs under control of the Microsoft Windows 10 operating system (OS), operators have access to 16,383 sequence steps in Tektronix's AWG Waveform Library. They can also generate complex waveforms by streaming instructions to each AWG via its dedicated Ethernet streaming ID connector, using combinations of the sequence steps. By selecting and combining different sequence steps, users can quickly create complex modulated communications signals, radar pulses, electronic warfare (EW), and electronic-countermeasures (ECM) waveforms, for almost instant modifications to even complex modulated waveforms. In addition, the software upgrade to the Windows 10 OS meets many corporate and government IT requirements.

FORGING WAVEFORMS

These AWG signal sources are suitable for a wide range of test applications, from commercial wireless communications systems and video systems to EW and military radar systems. They support the dynamic ranges needed to mimic real-world signal environments, with the ease of programming provided by the MS Windows 10 OS to create the most exotic and elaborate test waveforms.

The fast signal rise times of both AWGs *(see table)* makes them candidates for testing both defense-based and the rapidly emerging commercial radar systems helping to guide the growing number of vehicles equipped with advanced driver-assistance system (ADAS) electronic equipment. The single-channel model AWG70001B is capable of a signal rise time of 27 ps while the dual-channel model AWG70002B can generate pulses with rise times as fast as 22 ps/channel.

The speed and generous memory capacities of these AWGs support the dynamic signal-generation needs of defense-related applications, such as software-defined radios (SDRs). They also enable the synthesis of highly modulated waveforms, e.g., orthogonal-frequency-division-multiplex (OFDM) waveforms. By creating such advanced waveforms, it's possible to realistically characterize the


Mini-Circuits
USB/ETHERNET PROGRAMMABLE ATTENUATOR
Supports Dynamic Addressing (up to 25 units in series)
MODEL RCDAT-30G-30
0.1 – 30 GHz
0 - 30dB (0.5dB Step)
Serial Ctrl Out
Serial Ctrl In
USB
LAN
RF IN 50Ω
RF OUT 50Ω
MAX power: +35 dBm
NEW 30GHz

systems that use them. And by performing system-level measurements with such precise test signals, one can achieve high levels of transmission efficiency in both commercial and military communications systems where short transmission times must be relied upon to transfer a great deal of critical information.

The single-channel model AWG70001B can achieve maximum output frequency to 20 GHz while the AWG70002B offers two separate channels, each with maximum output frequency of 10 GHz. Both signal sources employ at least a pair of DACs with 10-b vertical resolution. Standard AWG70001B units are equipped with 2-Gsample waveform memory, with the option to extend the waveform memory to as much as 32 Gsamples. Similarly, standard two-channel AWG70002B AWGs come with 2-Gsamples waveform memory and can be equipped with as much as 16-Gsample waveform memory per channel (for the same 32-Gsample total). Both the single-channel AWG70001B and the dual-channel AWG70002B achieve SFDR of −80 dBc and operate at 1-ksample/s to 50-Gsample/s rates to support a wide range of output waveform synthesis.

When multiple-input, multiple-output (MIMO) and truly advanced signal-generation formats are needed, as many as four of the AWG70001B and AWG70002B AWGs can be synchronized together for high-speed in-phase/quadrature (I/Q) signal generation and to test phased-array radar systems. By using an AWG sync hub alongside as many as four AWG70000B AWGs controlled with SourceXpress PC software, the phase of the output signals can be maintained within a single clock cycle and tightly controlled within a phase adjustment range of ±10.800 deg. Any skew issues of the multiple output signals can be controlled within a skew adjustment range of ±10 ps for the multiple AWGs.

For advanced signal generation, especially for pulsed and complex modulated waveforms, these AWGs provide the power of the latest high-resolution, high-speed DACs under the control of the most up-to-date PC software. Whether as a single source of test signals or as many as four AWGs tightly synchronized together within the fraction of a phase degree, these AWGs provide the precision and resolution needed for testing SDRs, phased-array radars, and other military electronic systems. And they have the versatility to handle most types of modulation used in commercial high-speed, high-frequency systems. P&A: $83,600 and up; stock. Tektronix Inc., 14200 SW Karl Braun Dr., Beaverton, OR 97005; (503) 627-7111, www.tek.com.

JACK BROWNE | Technical Contributor

Software Tools Tackle Aerospace System Design

Computer-aided-engineering software tools such as MATLAB and Simulink allow EW and ECM system designers to model the effects of changes in design.

COMPUTER SOFTWARE orchestrates the operation of many defense systems, including electronic-warfare (EW) and electronic-countermeasures (ECM) systems, but can also aid in the design of multiple other types of systems. Software tools like MATLAB and Simulink from MathWorks allow system developers to practice model-based design (MBD) when developing their systems, to better understand their systems under different simulated operating conditions, and help reduce the overall design time.

The MATLAB and Simulink modeling tools are particularly useful in predicting the performance of electromechanical-system designs, in which the control of the system as well as the system itself must be modeled. To that end, MathWorks recently introduced (in its Release 2018b) Aerospace Blockset tools for the flight-control analysis of aerospace vehicles and Aerospace Toolbox capabilities for customizing the user interfaces of aerospace vehicle cockpit flight instruments.

These two software products provide different but complementary functions for aerospace and defense system designers. For those comfortable with expressing design ideas in terms of matrices and arrays, MATLAB is a math-based analysis program that can perform extensive analyses on a PC. It predicts how different algorithms will work with different bodies of data. When applied to larger network or "cloud" applications, the math analysis tool can scale as needed to prevent a computer from running out of memory when performing an extended analysis routine.

Simulink, on the other hand, is a software tool for simulating the performance of experimental and production systems under different and changing conditions, such as the demanding environments often faced by defense and aerospace systems. Simulink attempts to approximate what a real-world system will experience in a laboratory, without the long times of preparing the laboratory, the test equipment, and the test setups for each experiment.

For many designs, just having a software simulation version of a system can save countless hours in learning how that system might perform when facing arctic cold or desert heat—without having to recreate those environmental conditions in a laboratory. Because it's software, with a well-defined heritage and proven track record, users can combine different conditions (e.g., humidity, temperature, shock, and vibration) as part of a simulation without having to set up the physical equipment each time and receive simulated results.

In addition, Simulink can maintain traceability from initial requirements to the control code for a microprocessor when developing the control software for a complex system *(see figure)*. And, in many cases, it can automatically generate production-quality code for use by the microprocessors in a defense and aerospace system.

MATLAB and Simulink are supported by large code libraries and toolboxes. These allow users to "find" a function they may need for a more complex system without having to develop a software version of each function in a system.

To ease code development, algorithms developed and available in MATLAB can be added to a Simulink simulation as needed by applying the appropriate MATLAB code to a Simulink block. Existing toolboxes are available for a wide range of subsystems, including image processing, computer vision, and machine control, with new toolboxes being added to the product line on a regular basis.

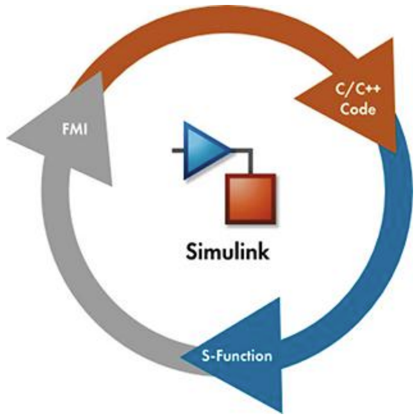

Simulink can maintain traceability from initial requirements to the control code for a microprocessor when developing the control software for a complex system.

One of the better-known systems that MATLAB and Simulink software helped in speeding the design process is the European Union's (EU's) Galileo satellite navigation system, an alternative to the U.S. satellite-based Global Positioning System (GPS). A software receiver for the Galileo Receiver Analysis and Design Application (GRANADA), which enables the integration of different receiver technologies within Galileo, was developed entirely through means of simulations within MATLAB and Simulink. de

MATHWORKS, 1 Apple Hill Dr., Natick, MA 01760-2098; (508) 647-7000, FAX: (508) 647-7001, www.mathworks.com.

Amplifier Powers 20 W from 70 to 500 MHz

MINI-CIRCUITS' ZHL-20W-52-S is a coaxial high-power amplifier capable of 20 W output power from 70 to 500 MHz. As well-suited for amateur radios as for military communications systems, it maintains typical gain of 50 dB with gain flatness within ±0.7 dB across the full frequency range. Based on silicon LDMOS power transistors, the rugged 50-Ω Class A amplifier is unconditionally stable with any kind of signal modulation, using patented technology (U. S. patent 7,348,854) to maintain constant current consumption (4 A at 24 V dc), and incorporating multiple protection circuits, including overvoltage and over-temperature protection (which shuts off the unit when the baseplate temperature exceeds +100°C). It's also reverse polarity protected and will not suffer damage with an open- or short-circuit output load under full CW output power operation. It has a typical noise figure of 7 dB and measures just 9.85 × 7.3 × 6.3 in. (250.19 × 185.42 × 160.02 mm) with SMA input and output connectors. The amplifier is designed for an operating temperature range of 0 to +65°C when used with the company's heatsink and fan.

MINI-CIRCUITS

P. O. Box 350166, Brooklyn, NY11235-0003; (718) 934-4500, https://www.minicircuits.com

Dual Directional Coupler Channels 0.7 to 6.0 GHz

MODEL C10117 is a dual directional coupler capable of handling 250 W CW input power from 0.7 to 6.0 GHz. Insertion loss is negligible, at 0.2 dB across the full bandwidth, with impressive coupling of ±1.0 dB or better. The coupler exhibits at least 15-dB directivity (typically 20 dB), maintaining high directivity under all load (mismatch) conditions. The typical VSWR is 1.30:1. Well-suited for accurately measuring forward and reverse power levels, the compact directional coupler measures just 2.00 × 2.00 × 1.06 in. and is available with numerous coaxial connectors, including Type N, BNC, and SMA connectors.

WERLATONE INC.

17 Jon Barrett Rd., Patterson, NY 12563; (845) 278-2220; E-mail: sales@werlatone.com, www.werlatone.com

Two-Way Divider/Combiner Cuts Loss from 8 to 18 GHz

MODEL 802-2-13.000 is a coaxial power divider/combiner rated to handle 30 W CW input power from 8 to 18 GHz. The worst-case insertion loss above the theoretical 3-dB power split is 0.6 dB. All output, power-combining ports are in phase, with worst-case phase difference of 5 deg. between ports, and all ports at a nominal impedance of 50 Ω. The amplitude balance is ±0.2 dB or better. The power combiner/divider exhibits maximum input VSWR of 1.35:1 and maximum output VSWR of 1.40:1. Minimum isolation between ports is 20 dB. The power divider/combiner, which is packed in a RoHS-compliant aluminum housing measuring 1.00 × 1.00 × 0.50 in., is supplied with female SMA passivated stainless-steel connectors that have gold-plated beryllium copper connector pins. Operating temperature range is –55 to +85°C.

MECA ELECTRONICS INC.

459 E. Main St., Denville, NJ 07834; (973) 625-0661, FAX: (973) 625-9277, E-mail: sales@e-MECA.com, www.e-MECA.com

Digital Variable Attenuator Controls 60 or 90 dB to 6 GHz

THE DA6 is a bidirectional digital variable attenuator capable of handling 0.3 W input power from dc to 6 GHz. Available as model DA6-60 with 60-dB attenuation range or model DA6-90 with 90-dB attenuation range, both 50-Ω units feature ±0.5-dB attenuation accuracy. Maximum insertion loss is 9 dB for the 60-dB attenuator and 13 dB for the 90-dB attenuator. Attenuation is adjusted in 0.5-dB steps with 100-ns switching speed for high-speed applications. Operating temperature range is –60 to +85°C. The RoHS-compliant variable attenuator measures 56 × 32 × 13 mm with stainless-steel SMA connectors per MIL-STD-348A. It can be supplied with a USB 2.0 interface as an option.

WEINSCHEL ASSOCIATES INC.

2505 Back Acre Circle, Mount Airy, MD 21771; (877) 948-8342, (301) 963-4630, FAX: (301) 963-8640, E-mail: sales@weinschelassociates.com, www.weinschelassociates.com

JACK BROWNE | Technical Contributor

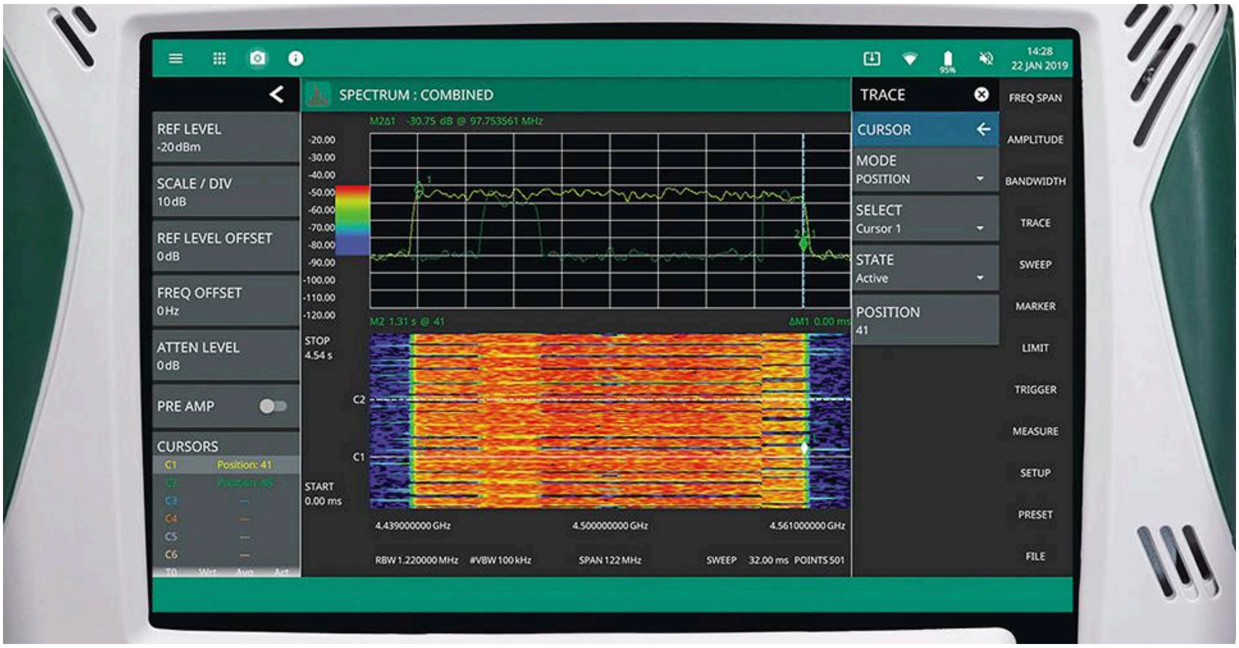

Portable Analyzers Take 5G Testing to the Field

These battery-powered spectrum analyzers provide instantaneous bandwidths as wide as 100 MHz from 9 kHz to 54 GHz with versatile display capabilities.

Portable spectrum analysis once meant a handle and sacrifice in measurement power compared to a larger benchtop or rack-mount spectrum analyzer. With the new Field Master Pro portable spectrum analyzer from Anritsu Co., there's no sacrifice. These portable model Field Master Pro MS2090A instruments put real measurement power in the palm of the hand—in seven frequency configurations from 9 kHz to 54 GHz.

The individual models cover frequency spans of 9 kHz to 9 GHz, 9 kHz to 14 GHz, 9 kHz to 20 GHz, 9 kHz to 26 GHz, 9 kHz to 32 GHz, 9 kHz to 44 GHz, and 9 kHz to 54 GHz. Those selecting one of the lower-frequency models can always send it back to the Anritsu factory (Morgan Hill, Calif.) for an upgrade to a higher frequency range.

These versatile spectrum analyzers leverage the latest analog and digital device technologies to provide wideband measurement capabilities that were possible only in a much larger rack-mount instrument. Depending on the measurement function, they provide at least 2 h of running time (and typically 3 h) on a rechargeable battery that fits within that handheld spectrum analyzer.

Even with their small sizes, the Field Master Pro MS2090A portable spectrum analyzers *(Fig. 1)* don't skimp on features. For instance, the display screen is a 10.1-in. diagonal color

The operating software menus for the Field Master Pro portable spectrum analyzers have been created and tested to follow industry standards for touchscreens and provide optimum user effectiveness. Operating modes and functions can be changed in less than five seconds to facilitate many different measurements in the field. As many as six separate traces can be shown on the display screen, with as many as 12 markers at one time.

touchscreen with 1280- × 800-pixel resolution. It offers adjustable brightness *(Fig. 2)* that makes it readily visible in bright sunlight and darkest night. The display screen has a "finger-swipe" function for simplicity, allowing users to swipe and scan across a trace to look for hard-to-find signals within a wide frequency range, or pinch on part of the screen to activate close-up views of signals of interest.

The operating software menus for the Field Master Pro portable spectrum analyzers have been created and tested to follow industry standards for touchscreens and provide optimum user effectiveness. Operating modes and functions can be changed in less than five seconds to facilitate many different measurements in the field.

As many as six separate traces can be shown on the display screen, with as many as 12 markers at one time. In addition, limit lines can be set for pass/fail readings. The display is protected by a rugged screen guard that can take the treatment of in-field testing; as evidence, the color touchscreen exceeds IK08 standards for lighting products for impact protection. Even connector ports are protected by rubber over-molds to ensure low loss and high measurement power in challenging operating environments.

POWERFUL PACKAGE

Behind that screen is some of the industry's most comprehensive signal-analysis measurement power. It's capable of a real-time spectrum-analysis bandwidth as wide as 100 MHz that, on the widest-bandwidth model, can be tuned anywhere within 9 kHz to 54 GHz. This type of portable measurement power supports many present and future test applications, including broadcast, defense, radar, satellite communications (satcom), and the inevitable 5G cellular wireless communications systems, both in the laboratory and in the field.

In terms of signal capture and display capabilities, these analyzers extend the limits for both large and small signals. The instruments all achieve a displayed average noise level (DANL) of better than −160 dBm with third-order intercept (TOI) of typically +20 dBm and phase noise of typically −110 dBc/Hz offset 100 kHz from the carrier. Regardless of captured signal power, the instruments maintain typical amplitude accuracy within ±0.5 dB.

1.Compact Field Master Pro MS2090A portable spectrum analyzers include a vivid 10.1-in. diagonal color touchscreen display with 1280- × 800-pixel resolution.

2. The large size of the display screen relative to the compact housing makes the Field Master Pro MS2090A spectrum analyzer a powerful field measurement tool.

3. The intelligent design of the Field Master Pro MS2090A analyzers includes top-mounted connectors, protected by a recessed cavity.

TESTING 5G

The portable spectrum analyzers have been designed with at least one major emerging wireless application in mind: testing the various signal components of the next version of cellular radio technology—5G New Radio (5G NR) wireless systems. Because of the steady consumption of radio bandwidth by wireless radio systems over the years, testing of 5G NR systems calls for an extremely broadband measurement system, including frequency bands at 3.5 GHz and in the millimeter-wave region at 28 and 39 GHz.

These analyzers handle tasks such as electromagnetic compliance testing, cell identification (ID) testing, beam ID testing, and measurements of spectral emission masks. On top of that, they feature enough instantaneous bandwidth for quickly locating harmonic and spurious signals and potential interference from other radio sources that will fall within the spectral region of 5G NR systems.

The Field Master Pro MS2090A analyzers combine hardware measurement power with software control to bring laboratory-like precision to the field. Their wide dynamic ranges and Spectrogram displays help simplify spectrum monitoring in the field, especially for spurious or occasional interference signals. Limit lines can be easily set for captured signals, to show such things as pass/fail signal levels.

As one application example, the wide capture bandwidth of these compact analyzers can be integrated with Anritsu's NEON MA8100A Signal Mapper software to make a 3D in-building map of signal coverage or a display of outdoor wide-area radio coverage by combining data captured with the MS2090A and the graphical display capabilities of the MA8100A software. In fact, the Field Master Pro MS2090A series includes a variety of automatic measurements to simplify in-field testing, including integrated channel power, occupied bandwidth (OBW) and adjacent-channel-power (ACP) measurements to simplify wireless communications system conformance testing.

Of course, 5G NR represents just one (albeit very large) future international wireless communications application. Motor vehicles will soon present another large application, both inside and outside the vehicles, as will everything plugged into the Internet of Things (IoT).

In addition to motor vehicles using radio waves to communicate to each other as part of the "smart highways" of the future, they will offer short-range radio waves, such as Bluetooth and wireless local area networks (WLANs) within each vehicle. As a result, passengers will be able to communicate with each other as part of what may eventually become a mobile WLAN, which will require the portability and the versatility of the Field Master Pro spectrum analyzers for on-site testing.

The analyzers themselves provide wireless connectivity by means of IEEE 802.11 and Bluetooth wireless standards, backed by the Global Positioning System (GPS) and Global Navigation Satellite System (GLONASS). Since more and more motor vehicles now include Universal Serial Bus (USB) connectors, the Field Master Pro spectrum analyzers also include USB 3.0 connectors as well as PCIe and Ethernet wired connections for physical interconnections to different equipment and instruments *(Fig. 3)*.

For those who remember the portable spectrum analyzers of years past, with their reliable measurement power but those large housings and blue handles, these spectrum analyzers are a fraction of the size and have considerably more measurement bandwidth. And that amazing 10.1-in. diagonal screen helps take the tedium out of high-frequency spectrum analysis. With its assortment of interconnecting ports, including USB 3.0, these little spectrum analyzers could even conceivably take on a USB test signal source in the field as part of a little "pocket-sized" test system that goes where needed. Plus, if 5G and vehicular wireless systems are any evidence, those test systems will be needed in the field. mw

ANRITSU CO., 490 Jarvis Dr., Morgan Hill, CA 95037-2809; (408) 778-2000, www.anritsu.com

IMS
Connecting Minds. Exchanging Ideas.
IMS2019
2-7 JUNE 2019
BOSTON 2019
THE HUB OF MICROWAVES
BOSTON CONVENTION & EXHIBITION CENTER
BOSTON, MASSACHUSETTS
Register Today!
For more information visit,
www.ims-ieee.org
IEEE
MTT-S
Get the entire pulse of the Microwave and RF industry in just a few days:
• The world's largest Microwave/RF component test & measurement, software and semiconductor exhibition featuring over 600 companies
• Over 75 technical sessions, workshops and panel sessions
• RF Bootcamp, a special course designed specifically for newcomers to the microwave world
• 5G Summit featuring experts from industry, government and academia
• Student forums such as design competitions, paper competition, PhD Initiative and Project Connect
• Special interest groups such as Women in Microwaves and Young Professionals
• Countless networking opportunities
• Special focus on startup companies with the first ever Startup pavilion, Startup panel session and Next Top Startup competition

FARRON L. DACUS | RF Design Consultant, Longwing Technology
www.longwingtech.com

Noise and its Shaping in Ultra-Low-Noise Synthesizer Design

This article, the third installment in a five-part series, dives into topics like noise transfer functions and total synthesizer noise.

This is the third article in our low-noise synthesizer design series. Part 1 (Dec. 2018) covered basic design for functionality and stability. Part 2 (Feb. 2019) explored the many noise sources in the synthesizer outside of the actual synthesizer integrated circuit (IC). This third article covers synthesizer IC noise, the closed-loop shaping of noises, and related issues such as optimum bandwidth and synthesizer IC figures of merit. A moderately more complete version will be published online, and still more detail is given in the full version at *www.longwingtech.com*.

This information allows for understanding of how modern synthesizers with on-die voltage-controlled oscillators (VCOs) have been able to displace discrete VCOs for many applications. It also explains when low-noise discrete VCOs offer advantages. Part 4 will review key parts and tools available to the low-noise synthesizer designer. The concluding Part 5 will present low-noise design examples, comparing on-die and discrete VCO results.

NOISE TRANSFER FUNCTIONS AND TOTAL SYNTHESIZER NOISE

Part 2 provided the main open-loop noise sources in the phase-locked loop (PLL). Now, we turn our attention to how these noises are shaped by the PLL into the closed-loop noise. We first present a generalized form, using the feedback tracking loop of *Figure 1*.

If we inject noise into any point "y" in the loop, and find the ratio of closed-loop noise on that node to the injected open-loop noise, we will get a generalized version of the highpass "error transfer function," $H_e(s)$, which was given in second-order form in the online version of Part 1:

$$\frac{Q_{nycl}}{Q_{ny}} = H_e(s) = \frac{1}{1+G_1G_2H} = \frac{1}{1+GH} \qquad (1)$$

Another critical function is the "closed-loop transfer function," CL(s), as described by Banerjee:

$$\frac{Q_{out}}{Q_{in}} = CL(s) = \frac{G_1G_2}{1+G_1G_2H} = \frac{G}{1+GH} \qquad (2)$$

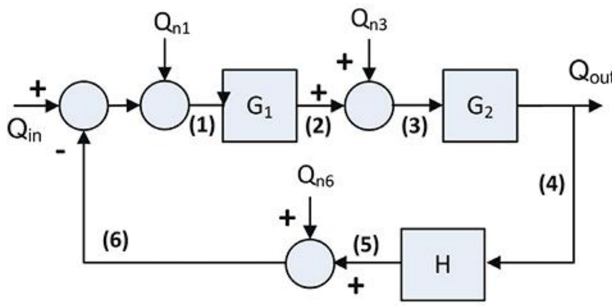

1. A generalized feedback tracking loop with noise "Q" injected at various spots is useful for deriving the noise transfer functions from a point "y" to a point "z." Here, the forward gain G is is broken up into G_1 and G_2 for generality.

This is similar to the classic "phase transfer function" given in older references, differing only as follows:

$$\frac{Q_6}{Q_{in}} = H_{classic}(s) = \frac{G_1G_2H}{1+G_1G_2H} = \frac{GH}{1+GH} \qquad (3)$$

Figures that illustrate $H_e(s)$ and CL(s) are shown in the full version of this article.

If we examine the noise from any point "y" into which we inject noise Q_{ny} into the loop, to an output node "z," where G_{yz} is the gain from point y to point z, we find:

$$\frac{Q_{nzcl}}{Q_{ny}} = \frac{G_{yz}}{1+G_1G_2H} = \frac{G_{yz}}{1+GH} = G_{yz}H_e(s) \qquad (4)$$

With this generalized information in mind, we may now consider the PLL block diagram of *Figure 2*.

The noise sources of this figure are:

- $\mathbf{V_{nx}}$**:** The steering input referred noise of the crystal reference oscillator itself, from its datasheet, as modified by the VCO noise modulation function to refer this oscillator noise to input.

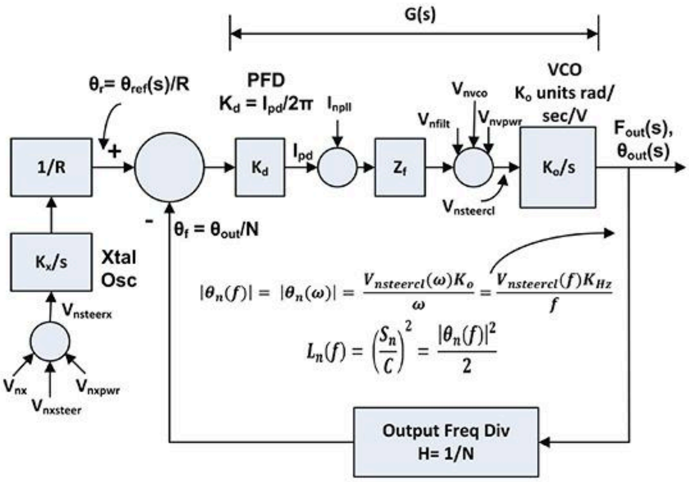

2. Shown is a general PLL block diagram with noise sources.

- **$V_{nxsteer}$:** The noise of the crystal steering input. Note that standard digital-to-analog converters (DACs) used for this function can be quite noisy.
- **V_{nxpwr}:** The input-referred noise from the crystal-oscillator power supply (see Part 2).
- **K_x:** Steering gain of the crystal reference in rad/sec/V. When referring noise to the xtal oscillator input, K_x should be converted to K_{xHz}.
- **I_{npll}:** The noise of synthesizer chip dividers and charge pump represented as a noise current, derived in the full version.
- **V_{nfilt}:** The output filter voltage noise density presented to the VCO steering input.
- **V_{nvco}:** The Leeson noise of the VCO referred to its steering input.
- **V_{nvpwr}:** The noise effect of VCO power-supply noise referred to the VCO input.

To make use of the transfer-function relationships derived above for the particular PLL case, we will need detailed filter functions. These are given in Table 1 of the full version on the Longwing website. With a particular filter designed and noise sources identified, we have what we need to find the closed-loop noise.

For the PLL block diagram with noise sources as given, we may write for forward gain:

$$G = K_d Z_f \frac{K_o}{s} = \frac{I_{pd}}{2\pi}\frac{K_o}{s} Z_f \qquad (5)$$

The voltage noise or noise sideband to carrier ratio (depending on whether the output node signal is variable in volts or in rad/sec) generated by noise "x" at point "y" is given by:

$$Q_{yz} = G_{yz} H_e = \frac{G_{yz}}{1+GH} = \frac{G_{yz}}{1+\frac{I_{pd}}{2\pi N}\frac{K_o}{s}Z_f} \qquad (6)$$

We may use this relationship with the input noises to generate the rms sum of closed-loop noises on the VCO input, and then the VCO noise modulation function to give the closed-loop phase noise on the output.

Using the "magnitude" function to emphasize these are rms noise quantities, the reference noise at the VCO input will be:

$$|V_{nxcl}| = \left|\frac{K_x}{s}\frac{1}{R} Z_f H_e\right| \qquad (7)$$

The noise from the charge pump and dividers of the synthesizer chip is normally handled directly at the VCO output using methods developed by Banerjee. These methods shall be presented later, but first we will develop the method of summing all noise sources to get total phase noise.

We assume here that we have a frequency-dependent current-noise function, i_{npll}, that can be summed into the loop filter. This noise-current function is derived from the Banerjee model in the full-length version. The noise voltage at the VCO input from the charge pump and divider noise is:

$$|V_{npllcl}| = |I_{npll} Z_f H_e| \qquad (8)$$

The closed-loop noises for the loop filter, input-referred VCO noise, and input-referred VCO power-supply noise are all on the VCO input, and are therefore simply the open-loop noises multiplied by H_e:

$$|V_{nfiltcl}| = |V_{nfilt} H_e(s)| \qquad (9)$$

$$|V_{nvcocl}| = |V_{nvco} H_e(s)| \qquad (10)$$

$$|V_{nvpwrcl}| = |V_{nvpwr} H_e(s)| \qquad (11)$$

Separately graphing each of these quantities over frequency is highly enlightening as to which terms are dominant, or worth more design effort and parts cost to reduce.

The magnitude of the total noise on the VCO steering input is given by the rms sum of the above sources:

$$|V_{nsteer}| = \sqrt{|V_{nxcl}|^2 + |V_{npllcl}|^2 + |V_{nfiltcl}|^2 + |V_{nvcocl}|^2 + |V_{nvpwrcl}|^2} \qquad (12)$$

Finally, this rms summed total noise voltage on the VCO input in the closed-loop state is transformed to a total output phase noise using the VCO modulation function.

CHARGE PUMP AND DIVIDER NOISE AND CORNER, SYNTHESIZER IC FIGURE OF MERIT, AND MODELING

This synthesizer IC charge pump and divider noise is often called "PLL noise," a term avoided here because confusion could arise as to whether this is total PLL noise. Instead, we use the term "CPD noise."

Flat Synthesizer Noise

First subjected to systematic deep analysis by Banerjee (Ref. 3), the physical source of this noise is the charge pumps and dividers, shaped by closed-loop action to often appear relatively flat over frequency. In recent years, this noise has dropped significantly.

We can intuitively understand this noise as follows. For any given pulse width with a given jitter, we can hypothesize that there will be a floor to this noise, a term proportional to the comparison frequency (number of the narrow pulses per unit of time), and a multiplication term similar to that of multiplying the crystal-reference phase noise. The resulting "flat" noise (neglecting 1/f at low-frequency offsets) is given by:

$$L_{flatdB}(f) = PN1HzdB + 20log|CL(f)| + 10log(f_{comp}) \quad (13)$$

Here, "PN1Hz" is the normalized floor on a per Hz basis. It's typically given in dB, but we will have occasion to convert it to linear. The empirical approach that supports this equation is proven in Ref. 4, in which a timing jitter analysis leads to the same results. Inside the loop bandwidth, **CL(f) ~ N**, and:

$$L_{flatdB}(f) = PN1HzdB + 20logN + 10log(f_{comp}) \quad (14)$$

Because $N = f_{out}/f_{comp}$, we may write:

$$L_{flatdB}(f) = PN1HzdB + 20log(f_{out}) - 10log(f_{comp}) \quad (15)$$

Since there's noise in each phase detector pulse, the 3-dB reduction of in-band noise for each doubling of f_{comp} in the above relation may seem odd. Doubling f_{comp} adds 3 dB to the noise contributed by the phase detector pulses. However, doubling f_{comp} also reduces N by two, which removes 6 dB of noise multiplication. The net is the 3-dB improvement shown.

This simple equation has powerful results for the synthesizer industry. We are normally given f_{out}, and by using a smaller N value, we get higher f_{comp} and lower in-band phase noise while generating that f_{out}. This is the method being strongly applied by semiconductor companies with modern sigma-delta fractional N synthesizers, with comparison frequencies now up to 100 to 200 MHz (Part 4) and high loop bandwidths. The high in-band noise suppression achieved is key to allowing higher-noise on-die VCOs to have effectively low noise at required phase noise offsets.

Flicker Synthesizer Noise

The method often used to model 1/f noise in the synthesizer chip is to assume that in-band noise at 10 kHz is dominated by flicker, and to scale that noise by output frequency relative to 1 GHz and by offset relative to 10 kHz. This gives:

$$L_{flickerdB}(f) = PN_{1-fdB} + 20log\left(\frac{f_{out}}{1E9}\right) - 10log\left(\frac{f_{off}}{1E4}\right) = PN_{1_{fdB}} + 20log(f_{out}) - 10log(f_{off}) - 140dB$$

(16)

The term PN_{1_f} is used by Analog Devices *(www.analog.com)* as a 1/f noise parameter. Texas Instruments *(www.ti.com)* refers to this same term as $PN_{PLL\_1/f}$. Linear Technology (acquired by Analog Devices) instead eliminates the referencing to 1-GHz carrier and 10-kHZ offset. They use the normalized 1/f noise term $L_{M(NORM\text{-}1/f)}$. Let's refer to this term with the simpler variables $PN_{flicker}$ and $PN_{flickerdB}$. Their equation is:

$$L_{flickerdB}(f) = PN_{flickerdB} + 20log(f_{out}) - 10log(f_{off}) \quad (17)$$

Comparing these two equations, it's seen that:

$$PN_{flickerdB} = PN_{1\_fdB} - 140dB \quad (18)$$

$$PN_{flicker} = \frac{PN_{1\_f}}{1E14} \quad (19)$$

Combining Flat and 1/f Synthesizer Noise

To add flat power to flicker power to get a total synthesizer chip noise power, we need linear terms, which are:

$$L_{flat} = PN_{flat} = PN1Hz\,|CL(f)|^2 f_{comp} \quad (20)$$

Within the loop bandwidth:

$$L_{flat} = PN_{flat} = PN1Hz\,N^2 f_{comp} \quad (21)$$

$$L_{flicker} = PN_{flicker}\frac{f_{out}^2}{f_{off}} = \frac{PN_{1-f}}{1E14}\frac{f_{out}^2}{f_{off}} \quad (22)$$

The total charge pump and divider noise at $f = f_{off}$ is given by:

$$L_{cpdtot} = L_{flat} + L_{flicker} \quad (23)$$

Assuming that the flicker corner is within the loop bandwidth, we may set the flicker and flat noises equal to solve for corner frequency at a particular output frequency, N, and f_{comp}. When we do this and substitute $N = f_{out}/f_{comp}$, we get as the closed-loop noise corner due to synthesizer IC 1/f noise:

$$f_{npllcorner} = \frac{PN_{flicker} f_{comp}}{PN1Hz} = \frac{PN_{1-f}}{1E14} \frac{f_{comp}}{PN1Hz} \qquad (24)$$

Current Noise Model

The above noises are expressed on the VCO output in the closed-loop state. Synthesizer CPD noise can be expressed as a sum of a flat and 1/f noise current injected into the loop filter in parallel with a then assumed noise-free charge-pump current. This form is useful for SPICE modeling of the synthesizer noise. The analysis to determine this noise is given in the full version. The results for the combined flat and 1/f noise are:

$$i_{nplltot} = \frac{\sqrt{2}\, I_{pd}}{2\pi} \sqrt{PN1Hz\, f_{comp}} \sqrt{1 + \frac{f_{npllcorner}}{f}} \qquad (25)$$

Synthesizer IC Noise Figure of Merit

If the square of the synthesizer chip noise current, $i_{nplltot}$, is integrated from 1 Hz to f_L, we obtain a synthesizer IC noise power figure of merit:

$$IC_{nfom} = \frac{I_{pd}^2}{2\pi^2} f_{comp} \left(PN1Hz\, f_L + f_{comp}\, PN_{flicker}\, ln(f_L) \right) \qquad (26)$$

Any time we are comparing two ICs with the same I_{pd} and f_{comp}, the figure of merit may be simplified to:

$$IC_{nfom} = PN1Hz\, f_L + f_{comp}\, PN_{flicker}\, ln(f_L) \qquad (27)$$

These figures of merit allow for comparing the total integrated in-band noise due to the synthesizer IC, taking into account variations in floor and corner that could disguise which IC may have the lowest total noise for a particular application.

OPTIMUM LOOP BANDWIDTH COUNTING ALL NOISE SOURCES

The "ideal bandwidth" generally means a bandwidth in which the typically nearly flat in-band noise intersects the VCO free-running noise at the loop bandwidth. A lower bandwidth would mean that the VCO noise at the loop bandwidth is higher than the flat in-band noise. It will look like significant noise peaking around the loop bandwidth as that noise is suppressed moving down into the loop bandwidth. A higher bandwidth will mean that the noise induced by the synthesizer IC will be higher than the VCO free-running noise at the loop bandwidth. These effects are shown in *Figure 3*.

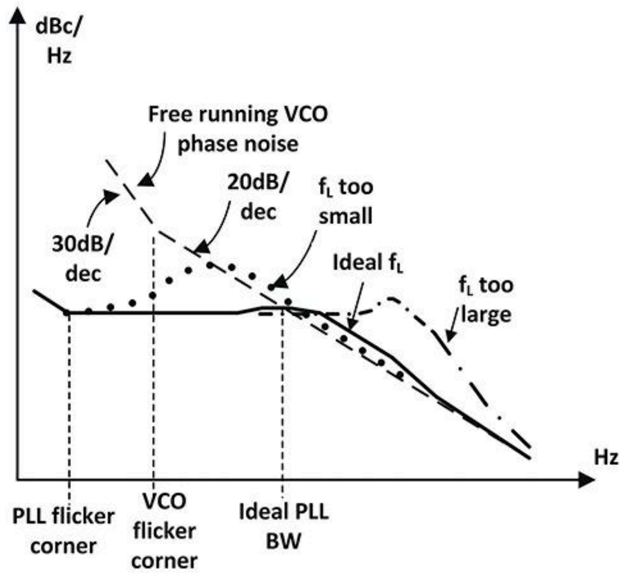

3. This is an illustration of ideal bandwidth versus noise effects of too small or large a bandwidth.

Ideal Passive BW for VCO Noise and Flat Synthesizer IC Noise Only

Ignoring any noise modulation of the VCO by the loop filter and the flicker corner of the synthesizer IC, we can easily find the approximate ideal bandwidth from setting $L_{flat} = L_{VCO}$ and solving for f. This is the approximate approach recommended by Banerjee (Ref. 3, 5th edition, pp. 305-306).

Assuming the desired f_L will be on the −20 dB/dec part of the phase noise slope, and that we know the phase noise $L(f_{ref})$, the VCO noise at a frequency f_L (the desired bandwidth) will be given by:

$$P_{nvco} = L(f_{ref}) \frac{f_{ref}^2}{f_L^2} = PN_{flat} \qquad (28)$$

The ideal bandwidth $f_{L\text{-}VCO}$, considering only VCO noise, then is:

$$f_{L-VCO} = f_{ref} \sqrt{\frac{L(f_{ref})}{PN_{flat}}} \qquad (29)$$

Ideal BW with the Passive Loop Filter Including Synthesizer and VCO Flicker Noises

We get a more accurate measure of the optimum minimum jitter bandwidth when these noise sources are considered. These noise sources may lead to either an *increase or decrease* in ideal bandwidth to that predicted using VCO noise alone. Adding loop-filter noises and VCO flicker noises will push out the ideal bandwidth. But, counting in the higher synthesizer IC noise with synthesizer flicker tends to push toward a lower intersection.

When we consider ideal bandwidth with the noise of a filter added to the VCO noise, in the frequency range where the bandwidth f_L will fall on the −20 dB/dec part of the VCO phase noise, and take into account synthesizer flicker noise, we may write:

$$P_{nvco} + P_{nfilt} = L_{flat} + L_{flicker} =$$

$$PN1Hz\, N^2 f_{comp} + PN_{flicker} \frac{f_{out}^2}{f_L} \qquad (30)$$

For the passive filter, the noise comes from the resistors in the filter. We are mostly interested in the noise at the loop bandwidth, where it's neither suppressed by the loop or filtered off by higher-order poles. At this frequency, using the thermal noise and the VCO noise-modulation function:

$$P_{nfilt} = \frac{M4kTR_2\, K_{Hz}^2}{2f_L^2} \qquad (31)$$

In this equation for P_{nfilt}, "M" is a multiplier for filter form. M = 1 for the first- and second-order filter (only R_2), M is generally about 2 to 3 for the third-order form (adding R_3), and generally about 3 to 4 for the fourth-order form (adding R3 and R4). Now, we can get a good approximation for R_2 from the second-order PLL equations, where:

$$R_2 \cong \frac{2\pi N f_L}{K_{Hz} I_{pd}} \qquad (32)$$

Substituting this into the equation for passive filter noise:

$$P_{nfilt} = \frac{M4\pi kTNK_{Hz}}{f_L I_{pd}} \qquad (33)$$

We may substitute this relation for P_{nfilt} and the linear expressions for P_{nvco} and P_{nflat} into Equation 31, and solve for ideal bandwidth f_L. Because the expression for P_{nvco} as a function of frequency is second order, the expression for P_{nfilt} is first order, and the expression for Pnflat is constant, we end up with a quadratic equation:

$$P_{nflat} f_L^2 - \left(\frac{M4\pi kTNK_{Hz}}{I_{pd}} - P_{nflicker} f_{out}^2 \right) f_L -$$

$$L_{vco}(f_{ref}) f_{ref}^2 = 0 \qquad (34)$$

Since this solution to this quadratic will always have a positive and negative frequency result, there's never any doubt as to the correct root.

Note in the above that it was assumed that the final bandwidth was at a frequency greater than the VCO flicker corner. This is often—but not always—true. If the final bandwidth calculated using the above is in fact below the VCO flicker corner, then we must modify our design procedure. This is shown in the full-length version, and results in a cubic relation for the bandwidth.

Ideal Bandwidth for the Slow Slew Active Loop Filter

This inverting form loop filter is the most recommended for higher-voltage-tune-range VCOs. An expression for the noise terms in the output of this filter was derived in the full-length version of Part 2 (Ref. 2). For the reasons given in the full-length version of this article, we may ignore the noise contributions of R_3 and R_4 when finding ideal bandwidth. Thus, the filter noises we use are:

$$V_{noptot}^2 = G_{n1}^2 V_{np}^2 + V_{nopR2}^2 + V_{nopInop}^2 \qquad (35)$$

Next, we translate this noise to VCO output using the VCO noise-modulation function, which gives:

$$P_{nfilt} = \frac{G_{n1}^2 V_{np}^2 K_{Hz}^2}{2f_L^2} + \frac{4\pi kTNK_{Hz}}{I_{pd} f_L} + \frac{i_{nop}^2 2\,\pi^2 N^2}{I_{pd}^2} \qquad (36)$$

We recall the VCO noise, including noise below its flicker corner as:

$$P_{nvco} = L(f_{cvco}) \frac{f_{cvco}^3}{f_L^3} + L(f_{ref}) \frac{f_{ref}^2}{f_L^2} \qquad (37)$$

The main equation to be used to set VCO and filter noise equal to synthesizer IC noise at the loop bandwidth f_L is:

$$P_{nvco} + P_{nfilt} = L_{flat} + L_{flicker} =$$

$$PN1Hz\, N^2 f_{comp} + PN_{flicker} \frac{f_{out}^2}{f_L} \qquad (38)$$

The above equations may be combined to give this equation cubic in f_L:

$$\left(\frac{2\pi^2 i_{nop}^2 N^2}{I_{pd}^2} - P_{nflat} \right) f_L^3 + \left(\frac{4\pi kTNK_{Hz}}{I_{pd}} - P_{nflicker} f_{out}^2 \right) f_L^2 + \left(\frac{G_{n1}^2 V_{np}^2 K_{Hz}^2}{2} + \right.$$

$$\left. L_{vco}(f_{ref}) f_{ref}^2 \right) f_L + L_{vco}(f_{cvco}) f_{cvco}^3 = 0$$

(39)

Here, the noise gain G_{n1} from op amp plus input to op-amp output at the loop bandwidth is given by:

$$G_{n1}^2 = \frac{V_{nopp}^2}{V_{np}^2} = \left| 1 + \frac{Z_{for}}{Z_{back}} \right|^2 \cong 1 \qquad (40)$$

The expressions for Z_{for} and Z_{back} developed in the full-length version of Part 2 may be approximated at f_L as below:

$$Z_{back} = R_3 + \frac{1}{sC_3R_3} = \frac{sC_3R_3+1}{sC_3} \cong \frac{1}{j2\pi f_L C_3}\ (at\ f_L) \qquad (41)$$

$$Z_{for} = \frac{1+sR_2C_2}{s(C_1+C_2+sR_2C_2C_1)} \cong R_2\ (at\ f_L) \qquad (42)$$

The above cubic relationship for f_L is to the author's knowledge the most accurate published relationship for getting an initial value for ideal loop bandwidth, as it takes all of the major factors into account. However, it still relies on several approximations, which are discussed in the full-length version along with more detailed analysis recommendations and a simplified version of this equation.

Ideal Bandwidth for the Semi-Active Buffered Loop Filter

The ideal bandwidth for this filter form is analyzed in the full version.

SPICE MODELING OF SYNTHESIZERS AND THEIR NOISE

The mathematical analysis is more flexible than SPICE, but it's quite a chore to juggle all of the noise sources and control system behaviors described above. A combination system (block) and circuit-level SPICE analysis can confirm the correctness of the mathematical analysis and can often be more accurate. Methods for using SPICE for PLL noise analysis are given in the full version.

SPUR NOISE

Spurs are discrete frequency components most commonly caused by digital noise on the phase detector output that get through the loop filter in at least noticeable form and cause modulation on the input of the VCO. These are discussed in the full version, and in greater detail in the references given there.

SYSTEM PHASE NOISE REQUIREMENTS

Approximate requirements for some applications are derived in the full-length version.

SUMMARY

This article has shown how the noise of the VCO can be significantly suppressed inside the loop bandwidth. Selecting the ideal loop bandwidth for the loop-filter type in use, and the synthesizer with the best figure of merit, will result in the lowest total integrated noise. Noise suppression with high-speed sigma-delta synthesizers allow even the noise of on-die VCOs to be suppressed to the point of now allowing fully integrated synthesizers for most applications (to be demonstrated in Part 5).

The long version of this article at *www.longwingtech.com* shows methods of synthesizer-noise specification that can show when an active loop filter and discrete VCO solution is necessary. mw

REFERENCES

1. "Design Methods of Modern Ultra-Low Noise Synthesizers," *Microwaves & RF*, Farron Dacus, Dec. 2018.
2. "Noise Sources in Ultra-Low Noise Synthesizer Design," *Microwaves & RF*, Farron Dacus, Feb. 2019.
3: "PLL Performance, Simulation, and Design," Dean Banerjee, first edition 1998. The 5th edition of 2017 of this outstanding reference may be freely downloaded at: *http://www.ti.com/tool/pll_book*.
4. Applied Radio Labs, application note DN006.

(Continued from page 22)

X50 would be used in 30 different devices to be released before the end of the year.

Many of these customers are also using Qualcomm's radio frequency front-end components that surround the main modem. They range from power amplifiers that convert signals from lower to higher power before sending them out through the antenna module, and filters that prevent interference from leaking into the front-end module—more commonly called the RFFE. These parts corral radio signals before feeding them into the modem.

Qualcomm is offering not only the cellular modem but also the antenna and other critical 5G components as an integrated solution, which it claims can cut the power consumption and enhance the performance of 5G devices. The company is trying to undercut other major players in the smartphone market, such as Broadcom, Qorvo, Murata and Skyworks. They sell many of the same components as Qualcomm—just not the modem.

RFFEs could be big business for Qualcomm, which set up a $3-billion joint venture with TDK in 2017 to build filters and other radio frequency parts. The market for front-end module components is forecast to more than double to $35.2 billion by 2023, according to market researcher Yole Développement. At the same time, though, the smartphone market's average annual growth is projected to be 2.5 percent through 2022, according to IDC.

"The need to support multimode operation from 5G to 2G, along with an ever-increasing number of band combinations, brings unprecedented complexity," Christiano Amon, Qualcomm's president, said in a statement. Integrating all these parts in the same smartphone is growing more difficult, and higher performance parts are required to support such a broad range of frequencies. "Discrete modem or RF solutions are no longer sufficient."

Part of the problem is that millimeter waves are blocked by hard surfaces, ranging from trees and concrete to windows and a person's hand. To support more advanced 5G networks, the signals are narrowed into beams and steered around obstacles. And that requires a complicated array of antennas and other parts. Suppliers have struggled to create chips small enough to fit into phones while limiting signal loss and overall power draw.

Qualcomm has started to untangle some of these snags. The company's third-generation antenna module, the QTM525, is designed with a more compact package than the previous QTM052. That enables it to fit into slimmer smartphones. The module adds the ability to access 26 GHz frequencies used in North America, Europe and other regions while keeping the QTM052's support for 28 GHz and 39 GHz bands used in Japan and South Korea.

The company also announced an adaptive antenna tuner that operates from 600 MHz to 6 GHz. The QAT3555 is designed to adjust the antenna's signal strength depending on its surroundings, limiting signal loss. The part's package is also 25 percent thinner than the previous generation's. The new QET6100 envelope tracking device supports 100 MHz bandwidths, which helps to cut on power consumption while boosting coverage and capacity. ■

Gain Equalizers Extend From DC to 20 GHz

MINI-CIRCUITS' EQY-XX-24+ family of microwave gain equalizers provides negative gain slopes with frequency to compensate for amplitude variations in amplifiers, receivers, and other electronic systems. Based on a highly repeatable GaAs MMIC semiconductor process, these 50-Ω equalizers feature broadband frequency coverage of dc to 20 GHz with nominal attenuation slopes of 0, 2, 3, 5, 6, 8, 10, and 12 dB. Supplied in a miniature 2- × 2-mm 8-lead MCLP package, the RoHS-compliant gain equalizers boast 20-dB typical return loss and low insertion loss across the wide frequency range. Model EQY-2-24+, for example, is a 2-dB gain equalizer with typical insertion loss of 3 dB at 10 MHz, 1.7 dB at 10 GHz, and 0.9 dB at 20 GHz, and 1.25:1 or better VSWR across the full frequency range. It handles input power levels to +31 dBm and has an operating temperature range of –55 to +105°C.

MINI-CIRCUITS, P.O. Box 350166, Brooklyn, NY 11235-0003; (718) 934-4500, https://www.minicircuits.com/WebStore/dashboard.html?model=EQY-2-24%2B

Torque Wrench Provides Precise Coaxial Connections

THE MINI-CIRCUITS MODEL TRQ-516-08 torque wrench enables highly repeatable, high-frequency, high-speed coaxial links with a wide range of RF/microwave connectors, including SMA, 3.5-, 2.92-, 2.4-, and 1.85-mm connectors. Using a head mechanism that breaks over when a preset torque value has been reached, the torque wrench prevents over- and under-tightening of coaxial connectors in test and system applications. The stainless-steel wrench, which is well-suited for applying precise connector mating forces in tight spaces, is calibrated to apply 8 ± 0.32 in.-lbs. (0.9 ± 0.04 N-m) of torque. It's light in weight at only 83.05 g, and only 6.44 in. (163.6 mm) long. The wrench is supplied in a kit with a wooden instrument case and calibration certificate.

MINI-CIRCUITS, P.O. Box 350166, Brooklyn, NY 11235-0003; (718) 934-4500, https://www.minicircuits.com/WebStore/dashboard.html?model=TRQ-516-08

LNA Quietly Boosts Automotive Applications

MODEL GRF2073-W is a low-noise amplifier (LNA) designed for high-volume, first-stage-amplification applications, including satellite-communications (satcom) systems, Global Positioning System (GPS) modules, and AEC-Q100 automotive-qualified amplifiers. Supplied in a miniature 2- × 2-mm DFN-8 package and well-suited for satcom receivers in the 2320- to 2345-MHz band, the amplifier covers 2.3 to 2.7 GHz with drain voltages from +2.7 to +5.0 V dc for typical gain of 20 dB. P&A: $1.25 (10,000 qty.); stock.

GUERRILLA RF INC., 1196 Pleasant Ridge Rd., Greensboro, NC 27409; (336) 510-7840, E-mail: sales@guerrilla-rf.com, www.guerrilla-rf.com

Skew-Matched Cable Pairs Link High-Speed Networks

A LINE OF skew-matched cable pairs exhibits less than 2-ps delay across 40- and 67-GHz bandwidths in support of high-speed networks and supercomputers. The delay-matched cables are available with 1.85- or 2.92-mm coaxial connectors and polarity indicators for matched cable ends. The skew-matched cable pairs feature VSWR of 1.40:1 and delay match as low as 1 ps. The flexible cable pairs are 100% tested for skew match.

FAIRVIEW MICROWAVE INC., (AN INFINITE ELECTRONICS BRAND),
301 Leora Ln., Ste. 100, Lewisville, TX 75056; (800) 715-4396, (972) 649-6678, www.fairviewmicrowave.com

Bidirectional Coupler Channels 150 W to 3 GHz

MINI-CIRCUITS' MODEL BDCH-25-33+ is a wideband, dc-pass bidirectional coupler for high-power applications from 800 to 3000 MHz. It maintains 25-dB typical coupling within ±1 dB across the full frequency range, with typical power-handling capability of 150 W. It features high typical directivity of 28 dB, with full-band insertion loss of typically 0.2 dB. The compact 50-Ω bidirectional coupler achieves 31 dB return loss for excellent impedance matching over the full frequency range. The bidirectional coupler, which passes as much as 2 A current, is designed into an open printed laminate measuring just 1.00 × 0.50 × 0.051 in. with wraparound terminations for good solder connections. RoHS-compliant and designed for operating temperatures from –55 to +105°C, the device is a good choice for monitoring high-power VHF and UHF radios and transmitters and in distributed antenna systems (DAS).

MINI-CIRCUITS, P.O. Box 350166, Brooklyn, NY 11235-0003; (718) 934-4500, https://www.minicircuits.com/WebStore/dashboard.html?model=BDCH-25-33%2B

Class AB Power Amp Drives 30 W to 6 GHz

MODEL 1219 is a solid-state Class AB power amplifier (PA) module. It provides at least 30 W and typically 40 W output power from 600 MHz to 6 GHz. Based on GaN-on-SiC device technology, the PA module is designed for +50-V dc power supplies. It provides typical small-signal gain of 61 dB with typical gain flatness of ±3 dB and has a gain adjustment range of at least 15 dB. It can handle input CW signals as large as +10 dBm without damage. Worst-case second harmonics are –15 dBc and worst-case third harmonics are –20 dBc. Spurious levels are –60 dBc or less. The amplifier module measures 7.0 × 4.0 × 1.1 in. and weighs 1.5 lb. with female SMA connectors. It's designed for operating temperatures of –40 to +85°C and meets the vibration and shock requirements of MIL-STD-810F.

EMPOWER RF SYSTEMS INC., 316 W. Florence Ave., Inglewood, CA 90301; (310) 412-8100, FAX: (310) 412-9232, www.EmpowerRF.com

Miniature Mixer Converts Signals from 700 to 2400 MHz

MODEL SFM-5 is a MESFET-based, high-third-order-intercept (IP3) frequency mixer with optimized RF range of 700 to 2400 MHz. With a local-oscillator (LO) range of 650 to 2000 MHz, it provides intermediate-frequency (IF) signals from 50 to 200 MHz with typical conversion loss of 10 dB and worst-case conversion loss of 11.8 dB. Fabricated with lead-free REL-PRO technology, the broadband 50-Ω mixer comes in a compact surface-mount housing with an operating temperature range of –20 to +70°C. The typical LO-to-RF-port isolation is 25 dB while the typical LO-to-IF port isolation is 20 dB. The broadband mixer is designed for use with nominal LO power of +17 dBm.

SYNERGY MICROWAVE CORP., 201 McLean Blvd., Paterson, NJ 07504; (973) 881-8800, www.synergymwave.com

Millimeter-Wave Connectors Link 110-GHz Bandwidths

A SERIES OF MILLIMETER-WAVE, removable end-launch printed-circuit-board (PCB) connectors includes components with bandwidths of 40, 50, 67, and 110 GHz and four different interfaces. The end-launch connectors are available as 16 models with increasing bandwidths for shrinking interface dimensions: 2.92 mm (40 GHz), 2.4 mm (50 GHz), 1.85 mm (67 GHz), and 1.0 mm (110 GHz). They are ideal for high-speed, serializer/deserializer (SerDes) applications such as supercomputers and high-speed networking. Though they exhibit VSWR as low as 1.10:1, the connectors don't require soldering and are reusable. In addition, a small profile with 0.35-in. mounting width allows for a high density of end-launch connectors in a small PCB area. The connectors, which have a stainless-steel outer conductor and gold-plated beryllium-copper center, contact are available in male and female versions. P&A: stock.

PASTERNACK ENTERPRISES, 17792 Fitch, Irvine, CA 92614; (978) 682-6936, (949) 261-1920, www.pasternack.com

This index is provided as an additional service by the publisher, who assumes no responsibility for errors or omissions.

Subscription Assistance and Information:
(ISSN 0745-2993)
Microwaves & RF is published monthly. Microwaves & RF is sent free to individuals actively engaged in high-frequency electronics engineering. In addition, paid subscriptions are available. Subscription rates for U.S. are $95 for 1 year ($120 in Canada, $150 for International). Published by Informa Media Inc., 9800 Metcalf Ave., Overland Park, KS 66212-2216. Periodicals Postage Paid at Kansas City, MO and additional mailing offices. POSTMASTER: Send change of address to Microwaves & RF PO Box 2100, Skokie, IL 60076-7800. For paid subscription information, please contact Microwaves & RF at PO Box 2100, Skokie IL 60076-7800. Canada Post Publications Mail agreement No. 40612608. Canada return address: IMEX Global Solutions PO Box 25542, London ON N6C 6B2.